



Contents lists available at ScienceDirect

Quaternary Science Reviews

journal homepage: www.elsevier.com/locate/quascirev

Postglacial environmental succession of Nettilling Lake (Baffin Island, Canadian Arctic) inferred from biogeochemical and microfossil proxies

Biljana Narancic^{a, *}, Reinhard Pienitz^a, Bernhard Chaplign^b, Hanno Meyer^b,
Pierre Francus^c, Jean-Pierre Guilbault^d

^a Laboratoire de Paléocécologie Aquatique, Centre d'études nordiques & Département de géographie, Université Laval, QC, G1V 0A6, Canada

^b Alfred Wegener Institute (AWI) Helmholtz Centre for Polar and Marine Research, Research Unit Potsdam, Telegrafenberg A43, 14473 Potsdam, Germany

^c Institut National de la Recherche Scientifique, Centre Eau-Terre-Environnement, Québec, QC, G1K 9A9, Canada

^d Musée de paléontologie et de l'évolution, Montréal, QC, H3K 2J1, Canada

ARTICLE INFO

Article history:

Received 26 June 2015

Received in revised form

9 November 2015

Accepted 21 December 2015

Available online xxx

Keywords:

Multi-proxy study

Postglacial reconstruction

Arctic

Marine/lacustrine transition

Sediment cores

XRF

Diatoms

Oxygen isotope

ABSTRACT

Nettilling Lake (Baffin Island, Nunavut) is currently the largest lake in the Canadian Arctic Archipelago. Despite its enormous size, this freshwater system remains little studied until the present-day. Existing records from southern Baffin Island indicate that in the early postglacial period, the region was submerged by the postglacial Tyrell Sea due to isostatic depression previously exerted by the Laurentide Ice Sheet. However, these records are temporally and spatially discontinuous, relying on qualitative extrapolation. This paper presents the first quantitative reconstruction of the postglacial environmental succession of the Nettilling Lake basin based on a 8300 yr-long high resolution sedimentary record. Our multi-proxy investigation of the glacio-isostatic uplift and subsequent changes in paleosalinity and sediment sources is based on analyses of sediment fabric, elemental geochemistry (μ -XRF), diatom assemblage composition, as well as on the first diatom-based oxygen isotope record from the eastern Canadian Arctic. Results indicate that the Nettilling Lake basin experienced a relatively rapid and uniform marine invasion in the early Holocene, followed by progressive freshening until about 6000 yr BP when limnological conditions similar to those of today were established. Our findings present evidence for deglacial processes in the Foxe Basin that were initiated at least 400yrs earlier than previously thought.

© 2016 Published by Elsevier Ltd.

1. Introduction

The need for better understanding of long-term climate and environmental variability in the Foxe Basin is due to the lack of high-resolution data from these remote and highly sensitive environments to major environmental changes (Ford et al., 2009; Rolland et al., 2008). Recent research efforts have been directed towards obtaining spatially and temporally dense proxy records of Holocene climatic change at high latitudes (ACIA, 2005; Alley et al., 2010; Kaufman et al., 2009, 2004; Smol et al., 2005). Nevertheless, high-resolution long-term climate records still remain scarce in these areas. The Foxe Basin and its surrounding regions have received little scientific attention compared to other parts of the Canadian Arctic, even though this region is of key importance to understanding the regionally very contrasting climate settings

since the last deglaciation. The Foxe Basin occupies a strategic position between areas undergoing drastic changes (High Arctic; Antoniades et al., 2007) and areas that exhibit more subtle changes (eastern Subarctic; Pienitz et al., 2003) over the course of the last millennium.

Lakes are important features of the landscapes in the Foxe Basin region. Lake sediments act as natural archives of past environmental change by accumulating biological remains from the lake and its catchment, as well as other non-biological materials originating from the surrounding environment and atmosphere. The majority of these lakes were formed after the last glacial retreat between ca. 18 000 and 6000 cal. BP (Dyke et al., 2002; Dyke, 2004) and contain valuable information about the regional postglacial development.

Although some Holocene paleoclimate reconstructions exist from Baffin Island (Axford et al., 2009; Briner et al., 2005; Joynt III and Wolfe, 2001; Thomas et al., 2011, 2008), high-resolution long-term climate records from the south-western part of the island are

* Corresponding author.

E-mail address: biljana.narancic.1@ulaval.ca (B. Narancic).

scarce, making it possible only to extrapolate roughly the regional postglacial climate history and landscape succession.

Here we used a multi-proxy paleolimnological approach involving elemental geochemistry from high-resolution μ -XRF analyses, diatom assemblage composition and oxygen isotope records from fossil diatom silica ($\delta^{18}\text{O}_{\text{diatom}}$) to study three sedimentary records retrieved from Nettilling Lake (Fig. 1) to reconstruct postglacial environmental changes of the lake basin. The results provide new data on the timing of the glacial retreat in the Foxe Basin and the duration of the postglacial marine invasion of the lake basin following glacial retreat. These records will complement existing and ongoing research of the postglacial dynamics in the Foxe Basin and on south-western Baffin Island.

While this study focusses on millennial paleoenvironmental succession of the lake basin, two recent studies provide information about 1) the recent (last ca. 1400 years) sedimentary processes of the plume region in the lake, controlled by glacial meltwaters (Beudoin et al., 2016, in review), and 2) about the paleohydrological evolution of the lake basin inferred from silica isotopes (Chapiligin et al., 2016, in review, this issue). Moreover, our multi-proxy study provides additional insights into both local- and regional-scale environmental and climate changes that have so far mainly relied upon palynological data in this part of the eastern Canadian Arctic (Jacobs et al., 1997; Wolfe et al., 2000).

The main objective of this research was to determine the timing of the glaciomarine-lacustrine boundary and to document paleoenvironmental changes that occurred over the postglacial period by integrating the information provided by sedimentary, geochemical and biostratigraphic markers.

2. Study area

Nettilling Lake, with an area of 5500 km², is the largest freshwater lake on Baffin Island and in the Canadian Arctic Archipelago. It extends from 65°53.767' N; 71°17.865' W to 66°59.569' N; 71°07.204' W (Fig. 1). The average depth of Nettilling Lake is about 25 m with a maximum depth of 60 m (Oliver, 1961). The western part of the lake basin is deeper ranging between 40 and 60 m, whereas the eastern part has an irregular and shallower basin with average depths between 10 and 25 m and numerous islands (Oliver, 1961). The lake is well mixed as no thermocline formation was observed in large parts of the lake (Chapiligin et al., 2016, in review, this issue). Based on field observations, lake ice is present until early August. The lake is located approximately 30 m above the present-day sea level (asl.; Jacobs et al., 1997; Oliver, 1961) and below the regional postglacial maximum marine limit of 93 m asl. (Blake, 1966). The surrounding landscape is of generally low relief apart from highland landscapes to the East. The western lowlands are made up of Ordovician carbonates, in contrast to the eastern highlands that are composed of Precambrian granites and gneisses overlain by Quaternary glacial, glaciofluvial and marine deposits. This contrasting geology has an influence on the terrigenous inputs to the lake. There are two major inflows to Nettilling Lake: the Isurtuq River brings in silt-laden meltwaters from Penny Ice Cap (67°15' N, 65°45' W; ~1930 m asl.) to the northeast, while Amadjuak River adds water from Amadjuak Lake (64°55' N, 71°09' W; ~113 m asl.) to the south of Nettilling Lake (Fig. 1). Nettilling Lake drains westward through the Koukdjuak River into the Foxe Basin.

Despite its large size (north-south extent: ca.120 km; west-east extent: ca.100 km), Nettilling Lake remains poorly studied. Some preliminary field investigations of its limnological characteristics were undertaken in 1956 by Oliver (1961). Jacobs and Grondin (1988) and Jacobs et al. (1997) focused on climate and vegetation characteristics of the southernmost part of the lake - Burwash Bay (Fig. 1) - revealing relatively mild summers and cold winters. Pollen

data provides evidence for regional climate control and influence on terrestrial productivity of southern Baffin Island in the past and today (Jacobs et al., 1997). A paleolimnological study by Beudoin et al. (2016, in review) reveals the direct influence of meltwaters from the nearby Penny Ice Cap on limnological and sedimentary structures and processes.

The Centre for Northern Studies at Université Laval (Québec, Canada) maintains a meteorological station with year-round automatic data acquisition at Nettilling Lake since 2010. Based on a four-year data set, mean July and January temperatures 7.3 °C and -26.7 °C, respectively. From general climatological considerations and extrapolation from coastal stations on the Canadian Arctic Islands, Maxwell (1981) inferred respective mean July and January temperatures to be 6.5 °C and -32 °C in the Nettilling Lake area, revealing a 5–6 °C increase in mean January temperature since the beginning of the new millennium.

Vegetation cover in the lake's catchment basin is sparse. Occasional botanical surveys during our field investigation revealed several low Arctic species including *Salix* sp., *Betula glandulosa* (dwarf birch shrubs), Ericaceae, *Carex* spp, *Eriophorum* sp. (wool grass), *Eriophorum scheuchzeri* (Scheuchzer's cottongrass), *Sphagnum* sp. (mosses), *Saxifraga rivularis*, *Saxifraga tenuis*, *Xanthoria elegans* (Sunburst lichen), *Stereocaulon* sp. (foam lichen), *Rhizocarpon* sp. (map lichen), *Ophioparma laponica* (bloodspot lichen) and *Peltigera canina* (dog lichen).

During the last glacial maximum (LGM), the Nettilling Lake region was covered by the Laurentide Ice Sheet (LIS). The Foxe Dome of the LIS expanded over almost all of Baffin Island with the exception of its eastern coast. At the onset of the Holocene, the Foxe Dome was still connected to the remainder of the retreating LIS. The gradual separation of the dome from the LIS was favored by the rapid penetration of marine waters into the Foxe Basin by ca. 8000 to 7500 ¹⁴C BP (Prest et al., Rampton, 1968; Barber et al., 1999; Miller et al., 2005). Based on Blake's findings (1966), the ice front retreated rapidly from Foxe Basin eastward across the Nettilling Lake basin towards Cumberland Sound and southward across the low eastern part of Foxe Peninsula to Hudson Strait, thereby leaving residual ice domes (remnants which are Penny and Barnes Ice Caps today) over central and northern Baffin Island (Miller et al., 2005). Disintegration of the Foxe Dome resulted in marine water invasion into the Nettilling basin at ca. 6600 cal. BP according to Blake (1966) and De Angelis and Kleman (2007). The current freshwater conditions were established by progressive glacio-isostatic uplift that led to the isolation of the basin from marine influence about ca. 5000 cal. BP (Blake, 1966; Fulton, 1975).

3. Methods

3.1. Field sampling

The three sampling sites were chosen based on the hypothesis that postglacial marine transgression and fresh water establishment would be preserved in the sediment records from the extreme opposite (west/east) sides of the lake. The Ni-MP core (104 cm) was taken in summer 2014 from the southern deep waters at 40 m depth and close to the central part of the lake (Fig. 1B). The Ni2-B (82 cm) was taken in spring 2012 from the north-eastern part of the lake at 14 m depth in the plume region where Isurtuq River brings in glacial melt water from the Penny Ice Cap. The Ni4-7 core (54 cm) was taken in the summer of 2010 from the shallower north-western lagoonal system at 3 m depth. Both these latter two cores were retrieved from the littoral zone. The fourth core Ni3-A (120 cm) was taken close to the sampling site of the Ni4-7 core and was only used to establish core chronology. At each coring site, the water depth was measured with a portable fish-finder sonar

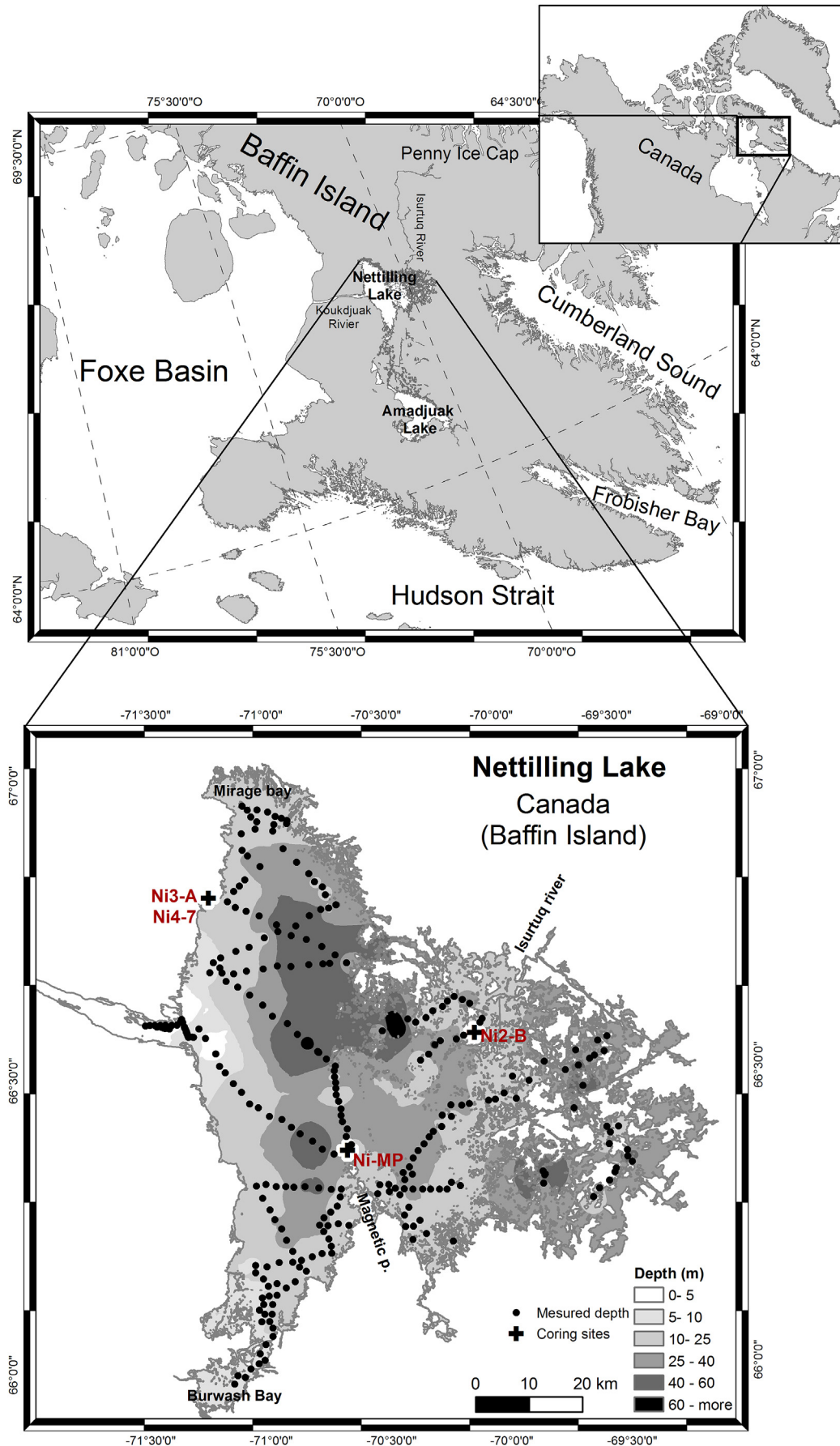


Fig. 1. Location of Nettilling Lake site on Baffin Island, Nunavut, Canada.

(Lowrance YSI 650MDS). A 7 cm-diameter handheld percussion corer (Aquatic Research Instruments) was used to collect the sediments. Sediment core lengths were limited by the presence of a compact glaciomarine clay unit underlying the lacustrine sediments.

3.2. Core chronology

The age-depth core chronology is based on 25 accelerator mass spectrometry (AMS) ^{14}C dates obtained on freeze-dried bulk sediments (5 measurements) from cores Ni-MP, Ni2-B and Ni4-7, *Hiatella arctica* (11 measurements) from Ni-3A, as well as three living aquatic plant samples taken from the lake shore at the respective coring sites in order to assess the potential reservoir-age effect (Saulnier-Talbot et al., 2009; Tables 2 and 3, Fig. 2a and b). Dates obtained from the aquatic plants were used to correct the dates obtained from other samples for potential old carbon contamination (Miller et al., 1999; Wolfe and Smith, 2004). Samples were picked and prepared at the Radiochronology Laboratory at Laval University, Québec (Canada) and measured at the Keck Carbon Cycle AMS Facility (University of California, Irvine, USA). The dates were calibrated using the program IntCal13 for bulk sediments and Marine13.14c with $\Delta R 615 \pm 20$ for seashell calibration (Vickers et al., 2010) with the software Calib version 7.1 (Stuiver et al., 1998).

3.3. Sediment core analysis

Sediment cores were cut lengthwise with a rotating saw and thin steel wire, and split in two halves. Split cores were covered with a plastic film and kept in a dark cold room to minimize surface oxidation and desiccation. The following parameters were measured using the working half-core:

3.3.1. Lithology

Loss-on-ignition (LOI) and water content. The working half-core was sub-sampled at 0.5 cm intervals. Sub-samples were freeze-dried for at least 24–48 h, depending on water content. LOI was performed on about 0.35 g of dry sediment at 550 °C for 5 h following the method of (Heiri et al., 2001) at 1 cm intervals to determine organic matter (OM) content (Fig. 3).

Grain size. Grain size analyses were performed on the residues from the LOI analysis at 1 cm intervals (Fig. 3). Approximately 0.02 g of sediment were mixed with a solution of sodium hexametaphosphate (10%). Subsequently, samples were analyzed with the Horiba laser particle sizer (McCave I. N. and Syvitski J. P. M., 1991) in the Laboratory of Sedimentology and Geomorphology at Laval University, Québec (Canada).

Magnetic susceptibility. The same half-sectioned core was analyzed for magnetic susceptibility (MS) at the Institut des Sciences de la Mer de Rimouski (ISMER) of the University of Québec in Rimouski, (UQAR, Canada). Measurements were done every 0.5 cm using a Bartington point sensor mounted on a GEOTEK multi-sensor core logger (Fig. 3).

3.3.2. μ -XRF

X-radiography and micro X-ray fluorescence (μ -XRF) core scanning analyses were performed at Institut National de la Recherche Scientifique (INRS-ETE, Québec, Canada) with an ITRAX core scanner on the second half-sectioned core in order to derive information on sedimentary elemental geochemistry. μ -XRF measurements were carried out at a downcore resolution of 0.2 cm with an exposure time of 40 s. Final results, given in peak area integrals for each element (dispersive energy spectrum), were normalized by the total counts per second of each spectrum (kcps) to take into account potential bias due to the irregular/heterogenic nature of

the sediment matrix (e.g., topographic variation of the core surface, water content and porosity; Fig. 4a and b; Bouchard et al., 2011; Cuven et al., 2011).

3.4. Analysis of bio-indicators

Diatoms. A total of 38 freeze-dried samples from Ni-2B (avg. 51.9 mg of freeze-dried material) and Ni4-7 (avg. 41.8 mg of freeze-dried material) core were cleaned following (Scherer, 1994) in the Aquatic Paleoecology Laboratory at Laval University, Québec (Canada). The clean siliceous material was subsequently mounted onto glass microscope slides with the synthetic resin Naphrax. Diatoms were identified and enumerated along random transects using a Zeiss Axioskop 2 microscope under phase contrast illumination at a magnification of 1000 \times . Between 300 and 500 valves were counted per sample in cores Ni-2B and Ni4-7 respectively. Broken cell walls consisting of more than half of the valve were counted as one valve. Diatom identifications were made to the lowest taxonomic level possible and the relative abundance of each identified taxon was calculated as the percent of the total number of valves. Results of the diatom analysis have been synthesized in the form of percentage diagrams (Fig. 5).

The ecology (salinity preferences) and taxonomic order presented in diagrams are based on various marine and freshwater floras (Krammer and Lange-Bertalot, 1986, 1988, 1991a,b; Snoeijs, 1993; Snoeijs and Vilbaste, 1994; Snoeijs et Potapova, 1995; Snoeijs and Kasperoviciene, 1996; Snoeijs and Balashova, 1998; Witkowski, 1994; Campeau et al., 1999; Witkowski et al., 2000; Fallu et al., 2000, 2005; Antoniadis et al., 2008). Salinity tolerances associated with the various diatom taxa are based on the simplified halinity (halobian) system proposed by Campeau et al. (1999).

Numerical procedures were conducted with the use of the R statistical software package v. 3.2.2 with the Rioja library 0.9-5 (Juggins, 2015). Rare taxa were removed from analysis. Only taxa with a minimum abundance of >4% and present in at least two samples were retained for core Ni2-B and >3% abundance in at least one sample in core Ni4-7. The different criteria allowed for downsizing higher number of valves per sample in Ni2-B core and they define the diatom assemblage of the most abundant diatoms. Biostratigraphic intervals were defined using a constrained cluster analysis with incremental sum of squares partitioning (CONISS).

Foraminifera. Six samples were taken from Ni2-B core for foraminiferal analysis: one in the glaciomarine phase (77 cm), four in the brackish phase (68, 61, 53 and 43 cm) and one from the lacustrine phase (33 cm). Samples varied in weight from 13 g to 5 g; they were wet-sieved through 1000 μm and 63 μm screens to eliminate, on one hand, large debris and on the other, silt and clay particles. The residue retained on the 63 μm screen included sand and foraminifera, plus similar-sized remains such as thecamoebian and tintinnid tests. Each sample was then rinsed in water, preserved and stored in air-tight plastic containers prior to qualitative identification by Dr. Jean-Pierre Guilbault at Musée de paléontologie et de l'évolution in Montréal (Canada).

3.5. Stable isotope analysis in biogenic silica

The 40 freeze-dried samples from the Ni2-B core were prepared for determining the oxygen isotope composition in siliceous diatom material (biogenic silica – SiO_2 ; Table 2). Previously published techniques were used that consist of a series of steps designed to chemically and physically remove non-diatom material from frustules (Chapligin et al., 2012a, b). The <10 μm fraction was used because it contained the most dominant diatom taxa for stable isotope analysis. Samples were chemically treated

Table 1

AMS ^{14}C radiocarbon dates obtained on samples from the four Nettilling Lake sediment cores Ni-MP, Ni3-A, Ni4-7 and Ni2-B and living aquatic plants collected at the respective coring sites.

Core ID/Location	Year collected	Depth (cm)	Material dated	Lab number	^b Modern fraction	Radiocarbon age (^{14}C yr. B.P.)	Calibrated age (cal. yr B.P.)	Deglacial reservoir age $\Delta R = 615 \pm 20$ (cal. yr BP)
Ni3-A	2012	12	<i>Hiattella arctica</i>	ULA - 3523	0.4522 ± 0.0010	6375 ± 20	7295 ± 36	6185 ± 82
Ni3-A	2012	18.5	<i>Hiattella arctica</i>	ULA - 3524	0.4433 ± 0.0010	6535 ± 20	7450 ± 26	6335 ± 65
Ni3-A	2012	20.5	<i>Hiattella arctica</i>	ULA - 3525	0.4447 ± 0.0009	6510 ± 20	7445 ± 29	6322 ± 69
Ni3-A	2012	26	<i>Hiattella arctica</i>	ULA - 3526	0.4458 ± 0.0010	6490 ± 20	7425 ± 13	6297 ± 79
Ni3-A	2012	34	<i>Hiattella arctica</i>	ULA - 3527	0.4359 ± 0.0009	6670 ± 20	7544 ± 37	6479 ± 90
Ni3-A	2012	36	<i>Hiattella arctica</i>	ULA - 3528	0.4338 ± 0.0009	6710 ± 20	7588 ± 24	6525 ± 93
Ni3-A	2012	45.5	<i>Hiattella arctica</i>	ULA - 3529	0.4323 ± 0.0009	6735 ± 20	7597 ± 27	6547 ± 89
Ni3-A	2012	54.5	<i>Hiattella arctica</i>	ULA - 3530	0.4255 ± 0.0012	6865 ± 25	7706 ± 54	6702 ± 90
Ni3-A	2012	59	<i>Hiattella arctica</i>	ULA - 3531	0.4321 ± 0.0009	6740 ± 20	7598 ± 26	6553 ± 89
Ni3-A	2012	78	<i>Hiattella arctica</i>	ULA - 3532	0.4036 ± 0.0008	7290 ± 20	8099 ± 69	7208 ± 64
Ni3-A	2012	106.5	<i>Hiattella arctica</i>	ULA - 5223	0.3939 ± 0.0008	7485 ± 20	8335 ± 39	7378 ± 68
Ni-MP	2014	1	Bulk sediment	ULA - 5054	0.7535 ± 0.0016	2275 ± 20	2326 ± 20	
Ni-MP	2014	31	Bulk sediment	ULA - 5055	0.5635 ± 0.0013	4605 ± 20	5312 ± 14	
Ni-MP	2014	61	Bulk sediment	ULA - 5056	0.5053 ± 0.0012	5485 ± 20	6292 ± 18	
Ni-MP	2014	88	Bulk sediment	ULA - 5053	0.5090 ± 0.0010	5425 ± 20	6244 ± 42	
Ni-MP	2014	101	Glaciomarine bulk sediment	ULA - 5052	0.4542 ± 0.0010	6340 ± 20	7282 ± 36	6131 ± 108
Ni2-B	2012	12.8	Bulk sediment	ULA - 4339	0.6075 ± 0.0013	4005 ± 20	4491 ± 31	
Ni2-B	2012	16.3	Bulk sediment	ULA - 4340	0.4442 ± 0.0011	6520 ± 25	7451 ± 35 ^a	
Ni2-B	2012	20.3	Bulk sediment	ULA - 4321	0.4492 ± 0.0012	6430 ± 25	7364 ± 59 ^a	
Ni2-B	2012	35.8	Bulk sediment	ULA - 4341	0.4690 ± 0.0012	6080 ± 25	6944 ± 64 ^a	5827 ± 88
Ni2-B	2012	68.8	Glaciomarine bulk sediment	ULA - 4320	0.5181 ± 0.0012	5285 ± 20	6057 ± 67	4896 ± 79
Ni4-7	2010	8.8	Bulk sediment	ULA - 1948	0.5257 ± 0.0009	5165 ± 15	5923 ± 18	
Ni4-7	2010	20.3	Bulk sediment	ULA - 1947	0.4957 ± 0.0008	5640 ± 15	6434 ± 37	
Ni4-7	2010	30.8	Bulk sediment	ULA - 1951	0.4811 ± 0.0008	5880 ± 15	6702 ± 37	
Ni4-7	2010	47.8	Glaciomarine bulk sediment	ULA - 1949	0.4560 ± 0.0008	6310 ± 15	7252 ± 18	6092 ± 93
Ni4-7	2010	52.8	Glaciomarine bulk sediment	ULA - 1950	0.2366 ± 0.0007	11 575 ± 25	13 401 ± 74 ^a	12 523 ± 104 ^a
Isurttuq River	2014	Surface	Aquatic plant	ULA - 5065	1.0561 ± 0.0020			
Mirage Bay	2014	Surface	Aquatic plant	ULA - 5066	1.0454 ± 0.0018			
Magnetic point	2014	Surface	Aquatic plant	ULA - 5067	1.0142 ± 0.0017			

^a Radiocarbon discarded from the age-model.

^b Modern fraction based on [Stuiver and Polach \(1977\)](#) conventions.

with H_2O_2 and HCl to remove organic matter and carbonates, respectively. Physical treatment included the heavy liquid separation with sodium-polytungstate solution for separating diatom material from clay particles (for details see [Chapligin et al., 2016](#), in review, this issue). Energy-Dispersive-X Ray Spectroscopy (EDS) under the scanning electron microscope (SEM) at the German Research Centre for Geosciences (GFZ Potsdam, Germany) was used to assess contamination. Contamination assessment followed mass-balance correction equations published in ([Brewer et al., 2008](#); [Swann and Leng, 2009](#); [Chapligin et al., 2012a](#)). From the sample set, 30 purified samples contained sufficient diatom material to be analyzed for $\delta^{18}\text{O}_{\text{diatom}}$ (Fig. 6). Inert Gas Flow Dehydration (iGFD, using Argon) technique has been used for removal of any exchangeable oxygen. This method consists of progressive heating of the diatom sample up to 1100 °C following continuous cooling under continuous Argon supply to outgas any exchangeable oxygen without reacting with the sample. Laser fluorination with bromine pentafluoride (BrF_5) was used to extract oxygen from the diatom frustules to be analyzed in a PDZ Europa 20-20 mass spectrometer ([Chapligin et al., 2010](#)). Any by-products were retained in a cold trap at a temperature of -196 °C while the liberated oxygen was transferred to the mass spectrometer and analyzed against reference oxygen of known isotopic composition. The final $\delta^{18}\text{O}_{\text{diatom}}$ was then calculated relative to the Vienna Standard Mean Ocean Water (V-SMOW) and expressed in ‰. For further methodological details, see [Chapligin et al. \(2010, 2011, this issue\)](#).

4. Results

4.1. Core stratigraphy

All cores used for establishing the chronology (Ni3-A, Ni-MP, Ni2-B and Ni4-7) consisted of three statistically significant biostratigraphic zones, determined through the CONISS: (1) bottom glaciomarine sediments, a coarse-grained sandy-silt diamicton, (2) mid-section laminated silt sediments, and (3) at the top, poorly to non-laminated lacustrine sediments. These zones corresponded well with the different salinity category that were identified based on the taxonomic composition of the assemblage. The Ni3-A core contains mainly glaciomarine sediments rich in macrofossil remains of *Hiattella arctica*, and it is for this reason that the Ni3-A core was used for age control in the composite age-depth models (Fig. 2). The Ni2-B core contains dropstones, pebble to gravel size, that likely are the remnants of ice-rafted debris (IRD). A distinct fine silt to sand laminated sediment interval separates the glaciomarine from the overlying lacustrine sediments. This interval is distinctively brown-colored in the Ni3-A and Ni4-7 cores, black in the Ni-MP core and gray-colored in the Ni2-B core. The upper lacustrine sediments are of a brown-olive color with alternating laminations of coarse-grained silt and sandy grains in all cores except for Ni2-B. The distinctively brown-orange coloration of this interval in core Ni2-B probably reflects iron-rich inputs from the Precambrian granite and gneiss highlands via Isurttuq River in the eastern part of the basin.

Table 2
Uncorrected and corrected $\delta^{18}\text{O}_{\text{diatom}}$ record from the $<10\ \mu\text{m}$ fraction. Highly contaminated samples (cont.) were excluded from the analysis. A correction was performed according to Al_2O_3 percentages and the difference between measured and corrected $\delta^{18}\text{O}_{\text{diatom}}$ values. $\text{SiO}_2\%$ and $\text{Al}_2\text{O}_3\%$ of the sample were determined by EDS (for more details see Chaplignin et al., 2012, this issue).

Sample depth (cm)	SiO_2 (%)	Al_2O_3 (%)	%Cont	$\delta^{18}\text{O}_{\text{measured uncorr.}}$ (‰) V-SMOW	$\delta^{18}\text{O}_{\text{corr.}}$ (‰) V-SMOW	$\Delta^{18}\text{O}_{\text{corr.}}$ (‰) V-SMOW
1.8	98.7	0.5	0.0	21.3	21.5	0.2
4.3	99.2	0.2	0.0	21.3	21.4	0.1
6.3	98.0	0.9	0.0	21.9	22.3	0.5
7.8	91.1	5.0	0.2	cont.	cont.	cont.
8.8	96.2	1.8	0.1	22.2	23.2	1.0
9.8	96.5	1.7	0.1	22.2	23.1	0.9
11.8	90.8	4.6	0.2	cont.	cont.	cont.
19.8	88.9	5.3	0.3	cont.	cont.	cont.
22.3	94.8	2.5	0.1	22.6	24.0	1.4
24.3	85.7	7.8	0.4	cont.	cont.	cont.
26.3	96.1	1.9	0.1	22.7	23.7	1.0
29.3	95.3	2.4	0.1	23.0	24.4	1.4
30.8	98.0	0.8	0.0	22.7	23.1	0.4
31.3	97.4	1.4	0.1	22.6	23.4	0.8
31.8	97.7	0.9	0.0	23.6	24.1	0.5
32.3	96.4	1.8	0.1	22.8	23.8	1.0
33.3	99.0	0.4	0.0	22.9	23.1	0.2
38.3	98.0	1.0	0.0	22.9	23.4	0.5
40.5	98.3	0.7	0.0	23.4	23.7	0.4
45.3	96.9	1.5	0.1	23.0	23.9	0.8
47.3	95.7	1.9	0.1	22.1	23.0	1.0
50.3	92.5	3.5	0.2	cont.	cont.	cont.
52.8	96.7	1.3	0.1	23.2	23.9	0.7
55.3	96.4	1.7	0.1	23.4	24.4	1.0
57.8	95.6	2.1	0.1	24.2	25.5	1.3
58.8	98.3	1.0	0.0	25.4	26.1	0.7
60.3	95.6	2.2	0.1	25.3	26.8	1.5
62.8	96.0	1.7	0.1	26.0	27.2	1.2
65.3	92.0	3.6	0.2	cont.	cont.	cont.
67.3	90.9	4.4	0.2	cont.	cont.	cont.
69.3	94.5	2.5	0.1	31.2	33.8	2.6
70.3	93.8	2.7	0.1	30.1	32.7	2.7
72.8	95.4	2.0	0.1	32.1	34.2	2.1
75.3	95.1	2.1	0.1	31.3	33.5	2.2
78.8	96.5	1.9	0.1	32.5	34.6	2.0
80.8	94.5	2.6	0.1	cont.	cont.	cont.
81.3	95.0	2.2	0.1	25.2	26.8	1.5
81.8	96.9	1.4	0.1	24.0	24.9	0.9

For more details see Chaplignin et al. (2016, in review, this issue) and Chaplignin et al. (2012).

Table 3
Water content and LOI percentage range in Ni-MP, Ni2-B and Ni4-7 cores throughout the stratigraphic phases.

Cores	Ni-MP				Ni2-B				Ni4-7			
	Water content		LOI		Water content		LOI		Water content		LOI	
	Min	Max	Min	Max	Min	Max	Min	Max	Min	Max	Min	Max
Lacustrine phase	42.7	51.0	4.4	8.3	29.0	49.1	5.1	9.7	42.1	56.2	5.1	8.5
Brackish phase	41.7	51.8	5.6	15.9	41.5	49.7	5.3	15.1	37.4	46.5	3.2	10.0
Glacio-marine phase	19.8	52.9	3.8	16.1	19.8	52.9	2.5	9.3	15.4	47.1	2.4	12.7

4.2. Core chronology

Dating of Arctic lacustrine sediments probably represents the most complex part of paleolimnological research in northern regions (Saulnier-Talbot et al., 2009; Wolfe and Smith, 2004). The lack of terrestrial carbon and the remobilization of old carbon stored in the permafrost of the catchment are often major challenges for the establishment of reliable radiocarbon-based lacustrine chronologies.

4.2.1. Reservoir age effect

The results of ^{14}C dates obtained on living aquatic plant material, bulk sediment and *Hiattella arctica* are summarized in Fig. 2a and b and Tables 2 and 3

Dated living aquatic plant material allowed to determine

whether or not the carbon stored in lake surface sediments and aquatic vegetation is in equilibrium with atmospheric $^{14}\text{CO}_2$ (Abbott and Stafford, 1996; Saulnier-Talbot et al., 2009). The average ^{14}C activity in the three aquatic plant samples was 1.0387 ± 0.0018 modern fraction (Table 1), indicating isotopic equilibrium (no reservoir effect). This means that the bulk sediment fraction from surface sediments of the Ni-MP core, which has a radiocarbon age of 2270 yrs, indicates a lag in deposition of terrestrial carbon to the lake bottom.

The radiocarbon dates obtained on glaciomarine bulk sediments and *Hiattella arctica* might have been influenced by deglacial marine reservoir age effects. A correction for the reservoir effect has been proposed by Vickers et al. (2010; $\Delta R = 615 \pm 20$; Table 1) for the eastern part of the Foxe Peninsula, with the additional remark that in this region the reservoir effect is not constant in time. Therefore,

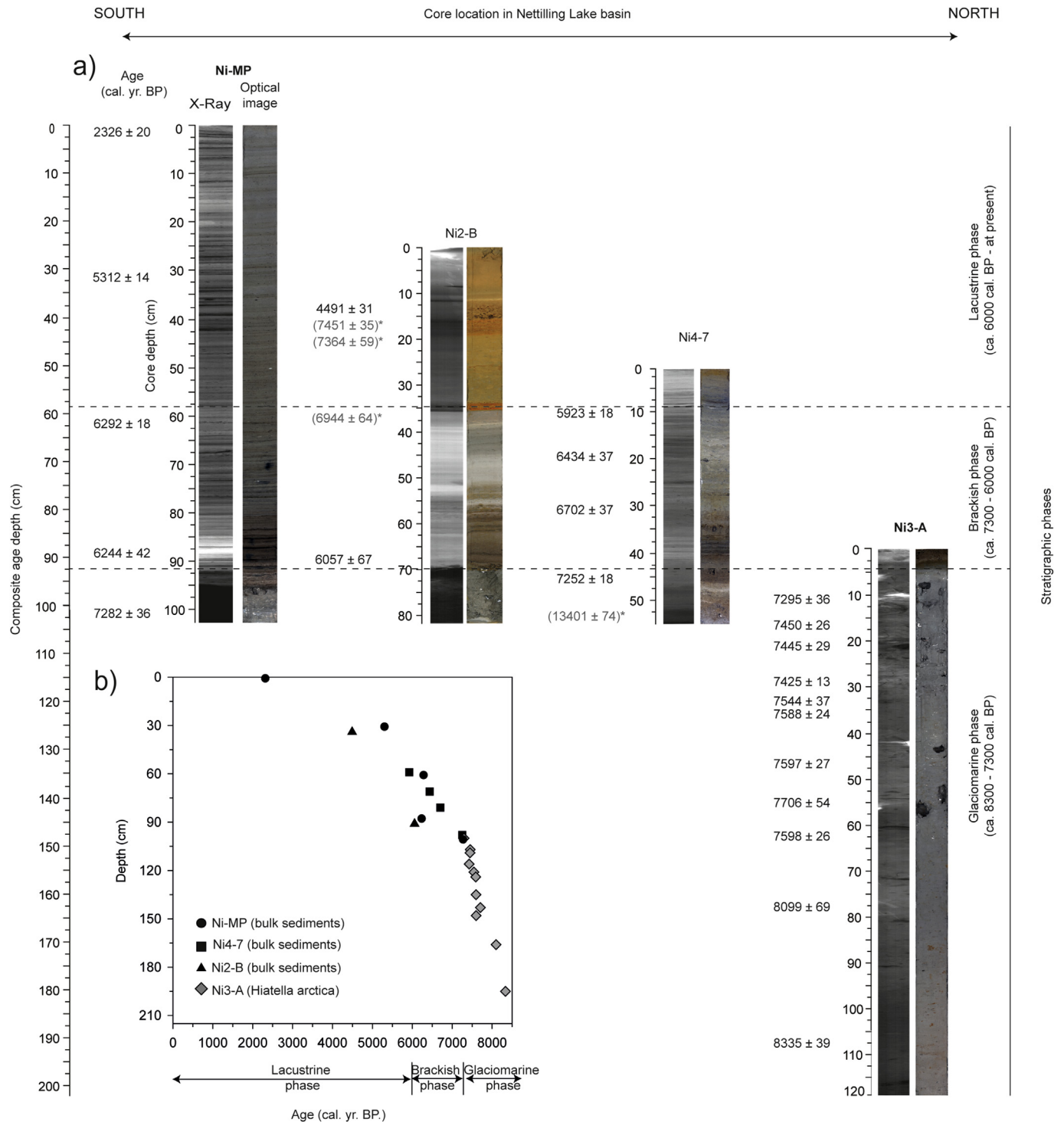


Fig. 2. (a) High resolution optical and x-Ray images of four cores (Ni-MP, Ni2-B, Ni4-7 and Ni3-A) with calibrated radiocarbon measurements and core location (south–north axis in the Nettilling Lake basin). Radiocarbon dates in gray are discarded from the age-model; (b) 210 cm long-composite age depth record is based on radiocarbon dates from bulk material (black filled symbols) and seashells (gray filled symbols). Corresponding time frame for each sedimentary phase: glaciomarine phase (ca. 8300 cal. BP- ca. 7300 cal. BP); brackish phase (ca. 7300 cal. BP- ca. 6000 cal. BP) and lacustrine phase (ca. 6000 cal. BP - present) yielded higher sedimentation rates in the southern part of the lake basin. *Old carbon admixture (for more details see section results 4.2 Core chronology).

in the composite-age depth model (Fig. 2) only calibrated ages are shown due to the absence of a full marine environment in the basin that furthermore was constantly being changed by freshwater inputs from the glacial melt of retreating ice fronts. Accordingly, it

becomes difficult to distinguish the proportion of fresh/marine water in the sediments. However, if the correction for the marine reservoir age effect were considered following Vickers et al. (2010), the glaciomarine sediments would be ca. 900 years younger.

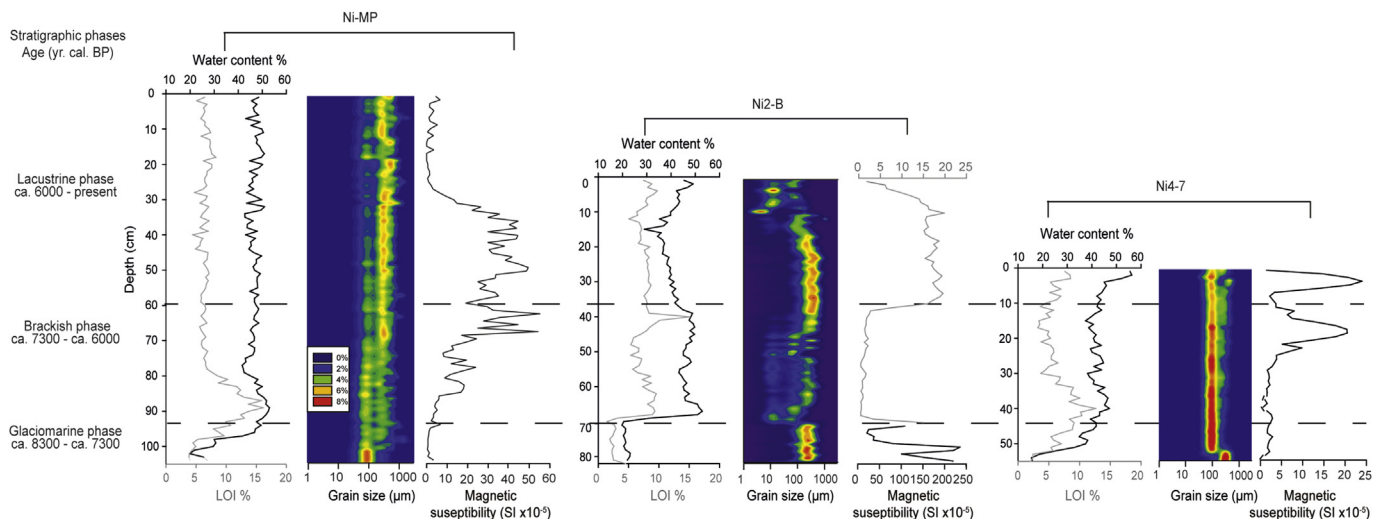


Fig. 3. General lithology for the cores Ni-MP, Ni2-B and Ni4-7. Water content (gray curve), loss-on-ignition, grain size and magnetic susceptibility are given for corresponding phases of Nettilling Lake basin development. Measured parameters in all three cores are showing similar trends for the corresponding phases with extremely low values for the glaciomarine sediment, high but decreasing values in brackish sediments and low and stable values for lacustrine sediments. However, measured magnetic susceptibility for Ni2-B core differs from this general observation.

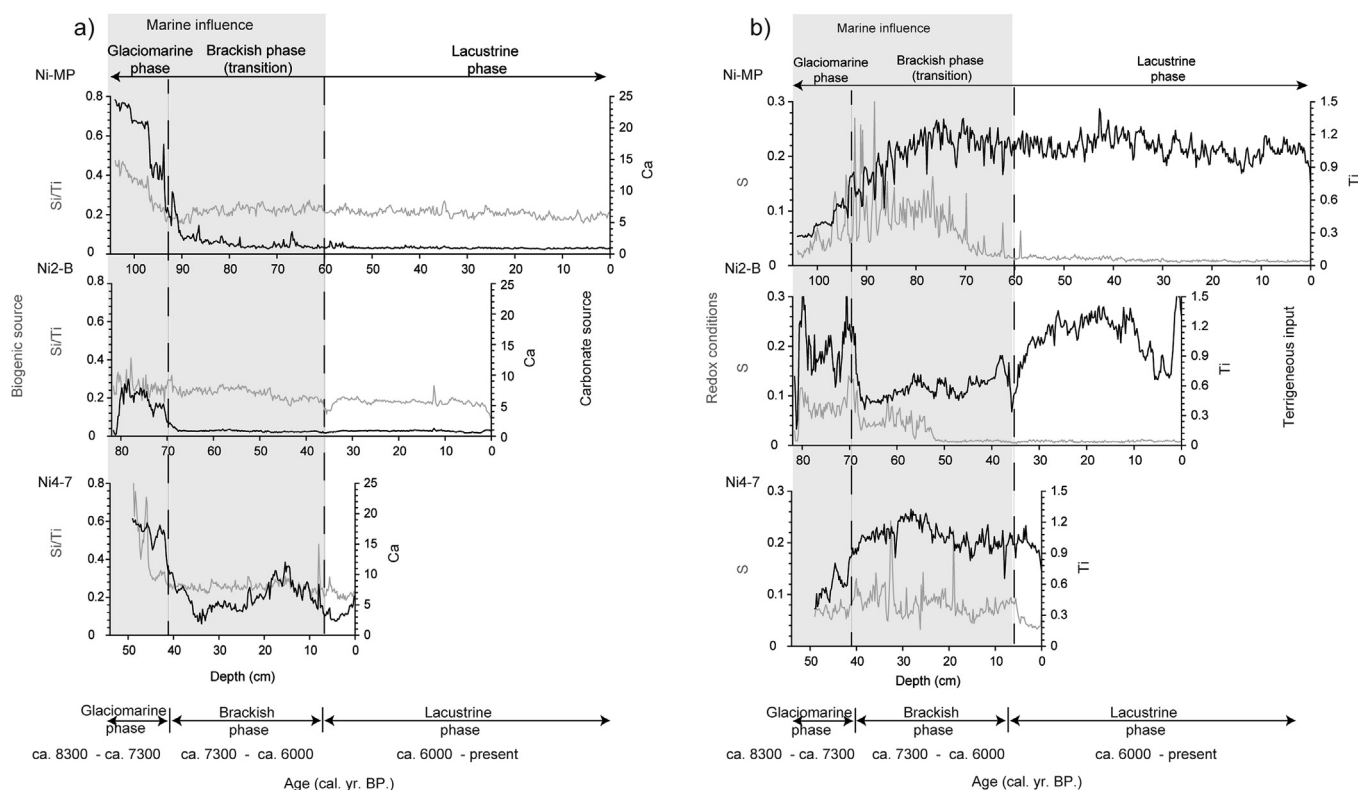


Fig. 4. μ -XRF results from three Nettilling sedimentary sequences (Ni-MP, Ni2-B and Ni4-7). Elemental profiles in peak areas are normalized by total counts per spectrum (kcps = 103 counts per second) at the corresponding depth. Increased Si/Ti (gray curve) and Ca (black curve) profiles indicate sediments rich in biogenic material from western carbonaceous terrain during the glaciomarine phase. Increased Ti (black curve) and S (gray curve) profiles indicate higher detrital inputs and anoxic conditions in the brackish sediments.

4.2.2. Age reversal

The age reversal in the lacustrine sediments of the Ni-2B core at 16 cm (7451 cal. BP), 20 cm (7364 cal. BP) and 35 cm (6944 cal. BP) could in part be explained by remobilization and transport of old carbon by Isurtuq River from the catchment and/or from the Penny Ice Cap meltwaters. Based on recent hydrochemical data

(Chapligin et al., 2016, in review, this issue), the Ni2-B core site is influenced by Isurtuq River water. However, recent hydrological regimes were likely different from those at the early stage of the lacustrine phase, when meltwaters from the Penny Ice Cap must have had a greater impact (Fisher et al., 1998, 2012; Zdanowicz et al., 2012). The subsequent retreat of the ice sheet to the northeast

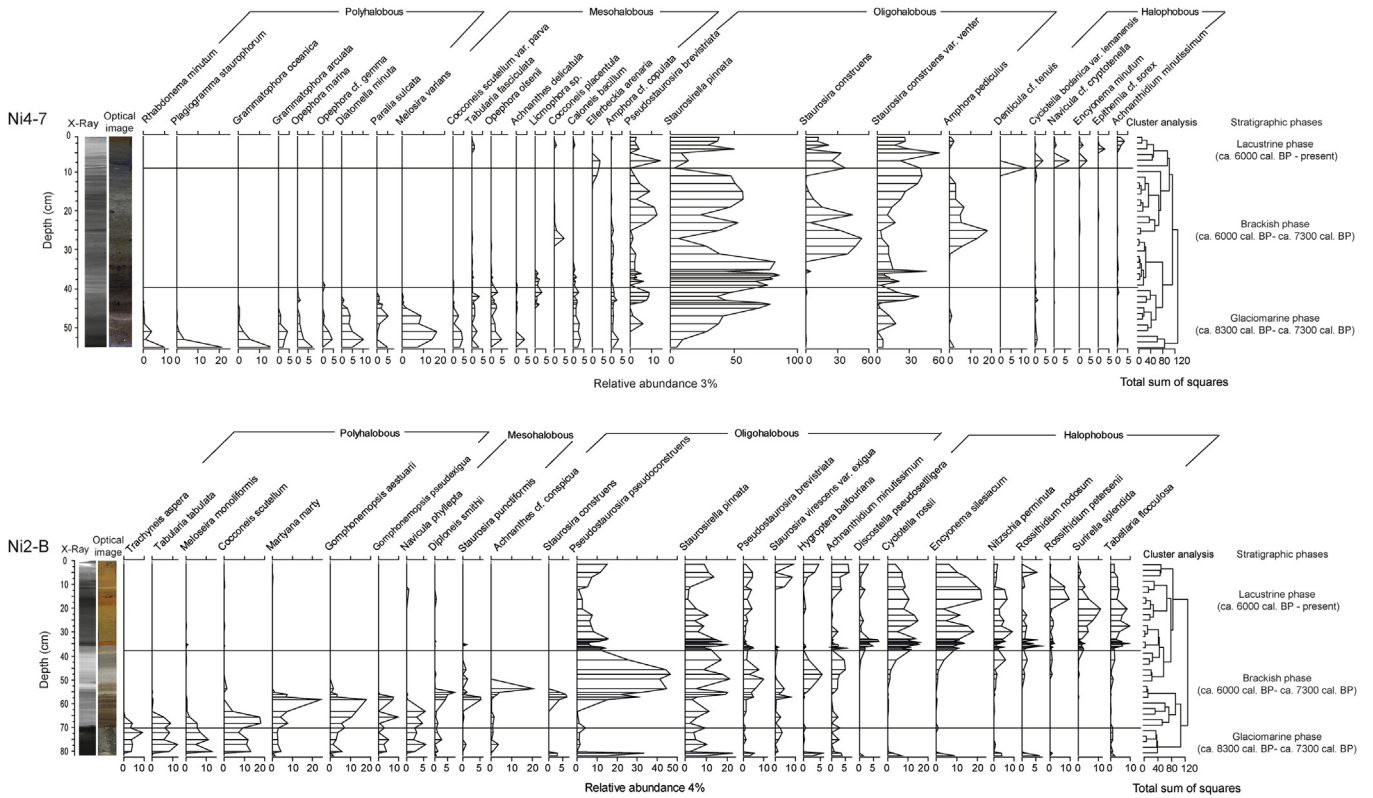


Fig. 5. Downcore changes in diatom assemblages in cores Ni2-B and Ni4-7 with X-ray and optical images of the cores. Diatom taxa are arranged according to salinity tolerances of polyhalobous and mesohalobous diatoms that are highly abundant in the glaciomarine phase, and on oligohalobous and halophobous diatoms in the brackish and lacustrine phases of the cores.

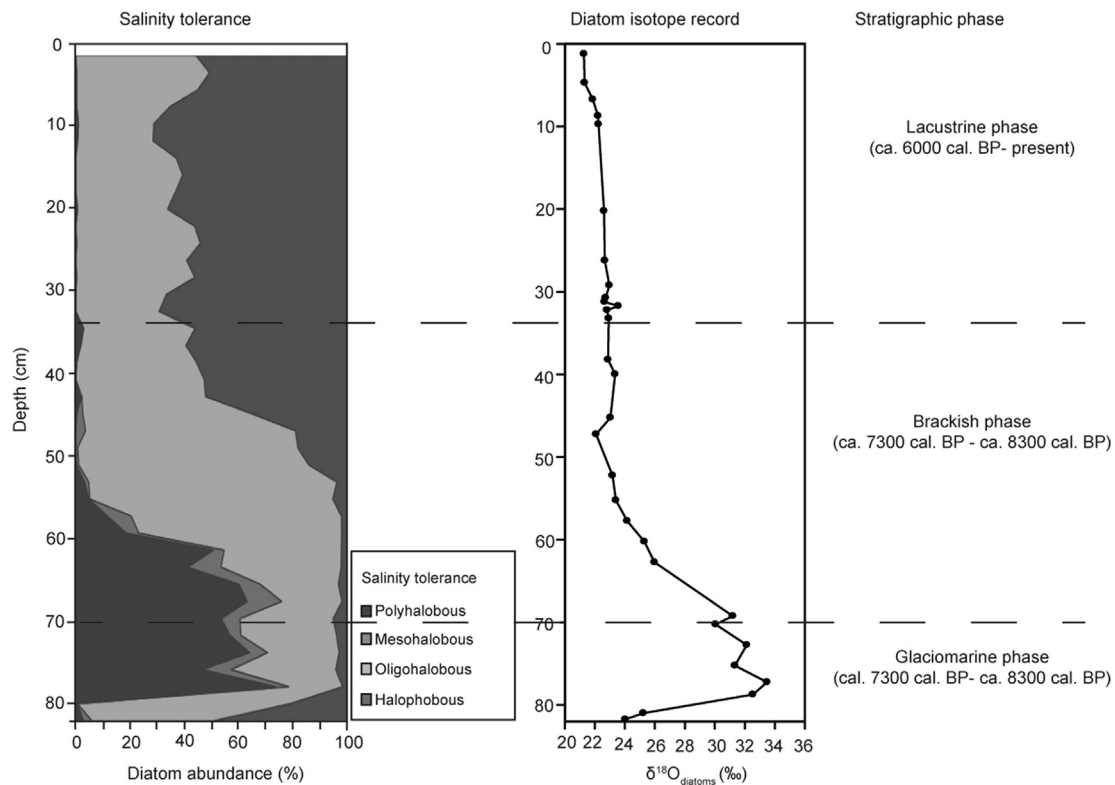


Fig. 6. Diatom salinity tolerance distribution throughout the Ni2-B core and corrected $\delta^{18}\text{O}_{\text{diatoms}}$ record from the fraction $< 10 \mu\text{m}$ show enriched oxygen isotope composition from diatom frustules associated to high salinity tolerance diatom: polyhalobous, mesohalobous and oligohalobous.

allowed older carbon to be liberated and transported to the lake, which explains the age reversals in this core. The absence of age reversals in the Ni-MP and Ni4-7 cores is likely due to their geographically distal and semi-disconnected position with respect to Isurtuq River inflow waters, thus being less prone to plume material inflow that might have triggered admixture of old carbon and date reversals in core Ni2-B. The 13 401 cal. BP date obtained from bulk sediments of the Ni4-7 core was discarded from the composite depth age models because it does not fit the overall general pattern of radiocarbon dates and yields an age when this region was likely covered by ice (Blake, 1966; De Angelis and Kleman, 2007; Dyke, 2004).

4.2.3. Composite age-depth model

The composite age-depth models was developed for four cores (Ni3-A, Ni-MP, Ni2-B, Ni4-7). Since the cores contain three recognizably concordant lithostratigraphic units, the overlap of these units as well as visual correlation of sedimentary cores were used to establish a composite core depth of 210 cm (Fig. 2). Based on radiocarbon dating and sedimentological changes, the four cores were divided into three stratigraphic zones with the corresponding time intervals: 1) the glaciomarine phase deposited between ca. 8300 and 7300 cal. BP, when the lake basin was inundated by postglacial glaciomarine waters of the Tyrrell Sea due to the glacio-isostatic depression of the crust; 2) the brackish water (transitional) phase and the beginning of basin isolation from marine influence between ca. 7300 and 6000 cal. BP and 3) the lacustrine phase that marks the complete isolation of the basin from glaciomarine waters and the establishment of the present-day lake conditions at ca. 6000 cal. BP.

4.3. Lithology

Glaciomarine sediments (ca. 8300–7300 cal. BP) had no macrofaunal remains with the exception of core Ni2-B where the Arctic sublittoral foraminifer *Trochammina cf. rotaliformis* occurred which is typical of low salinity marine environments (J-P Guilbault, pers. comm.). Water content and LOI values are the lowest in this section (Table 3, Fig. 3). Magnetic susceptibility is generally low and constant, except for the Ni2-B core with extremely high values (250×10^{-5} SI).

The brackish sediment layer (ca. 7300–6000 cal. BP) is characterized by higher water content and LOI than in the glaciomarine section of the cores (Table 3; Fig. 3). Magnetic susceptibility is still generally low except for the Ni-MP core where the gradual change from fine- to coarse-grained sediments through the glaciomarine-brackish water transition is paralleled by a gradual increase of magnetic susceptibility reaching its peak of 20×10^{-5} to 50×10^{-5} SI at the boundary between brackish and lacustrine sediments.

The upper lacustrine sediments (ca. 6000 cal. BP – present) of three cores are lithologically difficult to compare since they have different modern sedimentological settings. There is a significant difference in the amount of lacustrine sediments between the southern part of the basin close to the center of the lake (>59 cm; Ni-MP) and the northern part of the basin (only 9 cm; Ni4-7). The upper lacustrine sediments range from brown-olive (Ni-MP and Ni4-7) to brown-orange (Ni2-B) color with laminated silt to sand grains. However, some tendencies could be identified: water content and LOI are lower than in the brackish water sediments but do not reach the extremely low values of the glaciomarine phase (Table 3; Fig. 3). Magnetic susceptibility in this section shows relatively high values before gradually decreasing towards the top of the cores, particularly evident in the Ni-MP core with the longest lacustrine record.

4.4. μ -XRF

Major, minor and a few trace elements were detected by the ITRAX core scanner. Nettilling lake sediment contains 38 detected elements (Al, Si, P, S, Cl, Ar, K, Ca, Sc Ti, V, Mn, Fe, Co, Ni, Cu, Zn, Se, As, Br, Rb, Sr, Y, Zr, Nb, Mo, Tc, Ag, Sn, Sb, I, Cs, Ba, La, Hf, Pb, At, Ac) but most of those elements display noisy profiles. The most informative elemental profiles with the highest signal to noise ratio considered were Si, Ca, Ti and S in all the cores (Fig. 4a,b).

There are two potential sources of silicon in lacustrine sediments: terrigenous (quartz) and aquatic primary production (biogenic silica). Titanium (Ti) is often used as an indicator of terrigenous mineral inputs to lakes because of its presence in hard minerals that are less prone to weathering (Croudace et al., 2006). For this reason, Si/Ti ratios was used to infer contents of biogenic silica (Cuven et al., 2011). The carbonaceous bedrock and lowland terrain in the western part of the Nettilling Lake basin are rich in Ca, and therefore Ca was used to infer the initial shift in the dominant sediment source from carbonate-rich terrain in the West to granitic-gneissic terrain in the East. Furthermore, sea water is also richer in Ca than fresh water (Rolland et al., 2008). The Si/Ti and Ca contents were highest in the glaciomarine phase (ca. 8300–7300 cal. BP) and thereafter decreased progressively from the bottom to the top sediments of the lacustrine phase. The Ca values in core Ni4-7 were high in the brackish water phase (ca. 7300–6000 cal. BP) as compared to the decreasing trends in the other two cores; however, they did not reach the high levels measured in the glaciomarine phase sediments. Ti values increased throughout the Ni-MP and Ni4-7 core reaching their peak in the lacustrine phase. The Ni-2B core has the highest Ti values in the glaciomarine phase with again increasing values from the brackish towards the lacustrine phase. Furthermore, sulfur (S) was used as a paleoredox proxy, because sulfur concentrations usually increase in euxinic environments (Cuven et al., 2011; Retelle, 1986). The measured S values are very high in the brackish water phase and low in the lacustrine phase in all cores.

4.5. Diatoms and foraminifera

Selected taxa are arranged in order of salinity tolerances with polyhalobous (marine species with tolerance limit within the range 20 ppt–35 ppt), mesohalobous (brackish water species with an optimum range between 0.2 ppt–30 ppt), oligohalobous (indifferent taxa that thrive in both brackish and freshwaters) and halophobous (exclusively freshwater) taxa (Campeau et al., 1999). Fossil diatom assemblage analysis was performed on cores Ni2-B and Ni4-7 (Fig. 5). The three biostratigraphic assemblage zones were determined based on known salinity tolerances of the diatom species.

The glaciomarine sediments (ca. 8300–7300 cal. BP) were almost devoid of diatoms. The heavily fragmented specimens found in this section belong mostly to strongly silicified marine-neritic (littoral) forms, whereas fragments of less silicified fragile taxa were almost completely absent. These marine species belong to polyhalobous and mesohalobous benthic species, such as *Cocconeis scutellum*, *Martyana martyi*, *Gomphonemopsis aestuarii*, *Plagiogramma staur-ophorum*, *Grammatophora oceanica* and *Diatomella minuta*. According to Campeau et al. (1999), these species have salinity tolerances between 0.2 ppt and 35 ppt. These taxa even occurred beyond the glaciomarine sediment boundaries in the lower brackish water section up to 55 cm depth in core Ni2-B and up to 41 cm depth in core Ni4-7. The inwash of allochthonous material is indicated by the co-occurrence of a mixture of glaciomarine and brackish-freshwater diatoms such as oligohalobous *Staurosira pseudoconstruens* and *Staurosirella pinnata*, as well as the halophobous *Cyclotella rossii*

and *Encyonema silesiacum* in the bottom sediments of the Ni2-B core. Furthermore, glaciomarine sediments from this core also revealed a few dozen specimens of unidentified agglutinated foraminifera of the genus *Trochammina*, possibly *Trochammina rotuliformis*. Otherwise, only two unknown specimens of calcareous foraminifera were found, hence the fauna can be described as essentially monospecific. Because no modern analog of such a fauna is known from the Canadian Arctic (J.-P. Guilbault, pers. comm.) and given the taxonomic uncertainties, this foraminiferal assemblage must be considered paleoecologically non-diagnostic, apart from its affinity for a marine environment. However, the presence of the tintinnid *Tintinnopsis rioplatensis* Souto between 68 and 61 cm depth in Ni-2B is a clear indication of brackish water conditions according to (Scott et al., 2008). The upcore decline in foraminifer abundance is coincident with the decline in other marine indicators and the increase in freshwater fossils.

An increase in diatom species richness and a decrease in taxa associated with glaciomarine waters were observed in the brackish water phase (ca. 7300–6000 cal. BP), including some mesohalobous species but predominantly oligohalobous tycho planktonic *Fragilaria* spp. (e.g., *Staurosirella pinnata*, *Staurosira construens*, *Pseudostaurosira pseudoconstruens*, *Pseudostaurosira brevistriata*, *Staurosira construens* var. *venter*). Together, they represent 46–85% of the total diatom assemblage in this phase. The increasing number of oligohalobous forms coincides with a transition to brackish water conditions characterized by frequent fluctuations in salinity. Taxa belonging to *Fragilaria* spp. can tolerate salinities varying between 0 and 30 ppt (Campeau et al., 1999). The increasing abundance of oligohalobous forms upwards from 55 cm to 41 cm in cores Ni2-B and Ni4-7, respectively, with simultaneous decreases and the eventual disappearance of poly-/mesohalobous forms, confirms the overall trend towards increasingly freshwater conditions.

Lacustrine sediments (ca. 6000 cal. BP – present) contained assemblages mostly composed of halophobous diatoms between 36 and 0 cm in Ni2-B and 9–0 cm in Ni4-7. Freshwater species were most abundant and diverse in core Ni2-B. The dominant species in this section are *Encyonema silesiacum* and *Cyclotella rossii*. These are circumneutral oligotrophic benthic and planktonic freshwater species with variable abundances in the core that are described in more detail elsewhere (Narancic et al., in prep.).

4.6. Diatom isotope record

A strong variability in the diatom oxygen isotope composition is visible throughout the core Ni2-B with a minimum occurring at 2 cm depth and a maximum at 78 cm. Out of a total of 40 samples, 30 yielded enough diatom material with a purity of SiO₂ of more than 97.4% which were then further processed. The samples were corrected for contamination according to the formula used by Brewer et al. (2008) and Chapligin et al. (2011) to derive $\delta^{18}\text{O}_{\text{diatom}}$ for each sample.

The samples from the glaciomarine phase showed the highest isotopic composition reaching a mean value in $\delta^{18}\text{O}_{\text{diatom}}$ of +31.1‰ between 70 and 79 cm depth (N = 4; ca. 8300–7300 cal. BP; Fig. 6). However, measurements of $\delta^{18}\text{O}_{\text{diatom}}$ displayed relatively low values at the bottom of the core (+24.9‰ at 82 cm) as compared to the other isotopic measurements in the glaciomarine phase. A progressive depletion of $\delta^{18}\text{O}_{\text{diatom}}$ from +27.2‰ to +23.4‰ occurred within the brackish phase (ca. 7300–6000 cal. BP). The brackish phase is a transition zone with intermediate $\delta^{18}\text{O}_{\text{diatom}}$ values between glaciomarine and lacustrine $\delta^{18}\text{O}_{\text{diatom}}$. The $\delta^{18}\text{O}_{\text{diatom}}$ values are relatively low and stable throughout the lacustrine section varying between $\delta^{18}\text{O}_{\text{diatom}}$ +21.4‰ and +24.0‰. In comparison with the previous two sections, the $\delta^{18}\text{O}_{\text{diatom}}$ values

were lowest in the lacustrine phase and a gradual depletion of about 2‰ is visible towards the top of the core (+21.7‰ at 1.5 cm), where the maximum $\delta^{18}\text{O}_{\text{diatom}}$ is reached. According to Chapligin et al. (2016, in review, this issue), $\delta^{18}\text{O}_{\text{diatom}}$ of this most recent diatom sample corresponds well to the present-day $\delta^{18}\text{O}_{\text{lake}}$ of –17.4‰ at the coring position Ni2-B yielding a fractionation factor ($\alpha = 1.0410$) for the system diatom silica at Nettilling Lake. Taking into account the measured lake water temperature that ranged from 3.2 °C to 9.5 °C a theoretical isotope fractionation factor α was calculated for the system diatom silica-water of between 1.0445 and 1.0428 based on the formula from Leclerc and Labeyrie (1987) which is similar, but slightly higher than our calculations for Nettilling Lake. The $\delta^{18}\text{O}_{\text{diatom}}$ variability throughout core Ni2-B likely reflects hydrological changes, from isotopically enriched glaciomarine waters to isotopically more depleted freshwaters and may be used to infer paleosalinity changes in the lake basin.

5. Discussion

5.1. Paleogeographic and paleoenvironmental evolution of Nettilling Lake and surrounding landscapes

The paleoproxy records preserved in the sediment cores collected from different parts of the Nettilling Lake basin yield a scenario of glaciomarine sedimentation followed by progressive basin isolation and subsequent lacustrine deposition. The facies distribution and timing is glacio-isostatically controlled.

5.1.1. Glaciomarine phase (ca. 8300–7300 cal. BP)

Glaciomarine sediments accumulated in the basin while it was glacio-isostatically depressed. The gradual break-up of the Foxe Dome ice cap due to the warmer temperatures during the Holocene Thermal Optimum is characterized by low MS (Fig. 2) and low terrigenous inputs inferred from low Ti values (Fig. 4b). A low postglacial terrigenous input has also been reported from other Baffin Island lakes (Miller et al., 2005). However, this is not true for the Ni2-B core and this can be explained partly because the lake basin was proximal to the glacial meltwater outwash. Consequently, the presence of IRD in Ni2-B core probably brought in by glacial meltwaters yielded a strong MS signal compared to the overall trend for this period from other cores. Increasing LOI values in all three cores throughout the glaciomarine section indicate enhanced primary production due to higher summer temperatures and longer duration of the open water season. High Si/Ti ratios in glaciomarine sediments of the three cores (Fig. 4a) are associated to biogenic silica contents and/or to inorganic silica from the weathering of the surrounding rocks by glacial meltwaters, thus associating these high ratios in part to inorganic silica and not exclusively to biogenic silica (Beaudoin et al., 2016, in review).

The predominance of polyhalobous oceanic diatoms in Ni2-B and Ni4-7 cores indicates that the immediate and initial postglacial history of the Nettilling Lake basin was under marine influence. This is also evidenced by the relatively high $\delta^{18}\text{O}_{\text{diatom}}$ values in Ni2-B core of about +31‰ during the glaciomarine phase in the isotope record (Fig. 6). It must, however, be stated that these are not fully marine conditions yet likely displaying the influence of glacial melt. This is further substantiated by the presence of benthic estuarine taxa in Ni4-7 core such as *Rhabdonema minutum* and *Plagiogramma staurophorum* in the western part of the basin typical of a shallow and weakly saline marine environment influenced by high freshwater inputs from the melting glacial front (Poulin et al., 1984a,b,c). The overall abundance of benthic forms with wide salinity tolerance and the almost complete absence of planktonic marine species indicate a shallow and dynamic nearshore

environment. The presence of the bivalve *Hiatella arctica* in Ni3-A used for ^{14}C dating further supports a low intertidal environment where a small and marginal community of these bivalves lived (Retelle, 1986). However, when looking at the three cores' sediment fabric (lithology), some discrepancies are obvious especially with regard to the Ni2-B core. High MS, predominantly fine sands to silts with abundant IRD, low primary production and water content in Ni2-B core, suggest intensification of glacial erosion and higher inputs of glacially eroded sediments into the basin (Miller et al., 2005). Few fragmented benthic taxa found in this section of Ni2-B core, such as *Tabularia tabulata*, *Cocconeis scutellum*, *Navicula phyllepta* and tychoplanktonic taxa indicate a very dynamic glaciomarine environment.

The glaciomarine environment in the eastern part of the lake basin was probably more proximal to the glacier margin and dropstones and other coarse-grained materials in Ni2-B core likely were deposited by glacial meltwaters. This part of the basin is today still influenced by glacial meltwaters from the Penny Ice Cap. Most likely, an early stage with enhanced freshwater inputs is also visible in the isotope record as indicated by the relatively high $\delta^{18}\text{O}_{\text{diatom}}$ values at the beginning of the glaciomarine phase (Fig. 6). This is further substantiated by the diatom assemblages as well as the $\mu\text{-XRF}$ data. The radiocarbon dates obtained from *Hiatella arctica* in Ni3-A core (Table 1; Fig. 2) suggest that the ice margin had receded from the head of the eastern Foxe Basin coast west of present-day Nettilling Lake by ca. 8300 cal. BP. Blake (1966) argued the time interval for the Foxe Basin ice retreat to be between 6800 and 6700 ^{14}C , whereas Dyke placed this time interval between 7000 and 6500 ^{14}C BP and De Angelis and Kleman (2007) between 7000 and 6000 ^{14}C BP. Most of these dates from the above mentioned studies were extrapolated. However, our radiocarbon dates are the first to be measured *in situ* from Nettilling Lake sediment cores. Even if a marine reservoir effect were included to our data (see results section; $\Delta 615 \pm 20$ yrs; Vickers et al., 2010) yielding a maximum age of ca. 7400 cal. BP for the marine phase, we are confident in suggesting that Foxe Basin deglaciation happened a few hundred years (ca. 400 yrs) earlier than previously thought.

The gradual transition from the massive glaciomarine to micro-laminated fine-grained sediments in the cores coincides with lake basin emergence due to the glacio-isostatic rebound from the postglacial sea which, based on our dates, occurred between ca. 8300 and 7300 cal. BP. Our data provides no additional evidence for a temporary marine pathway and intrusion from the east, i.e. via the Cumberland Sound as suggested by Blake (1966).

5.1.2. Brackish water phase (ca. 7300–6000 cal. BP)

The transitional brackish water section is characterized by decreasing marine influence and increasing terrestrial runoff between ca. 7300 and 6000 cal. BP. Primary production rises in this section possibly due to the expansion of tundra vegetation in the lake catchment area in response to climate warming during the Holocene Thermal Optimum in eastern Canadian Arctic. Enhanced freshwater inputs from melting glacier fronts lead to an $\delta^{18}\text{O}$ depleted isotopic composition in the lake as evidenced by decreasing $\delta^{18}\text{O}_{\text{diatom}}$ values from $+27\text{‰}$ to $+23\text{‰}$ in Ni2-B core (Fig. 6). The predominant diatom species in this section of the Ni2-B and Ni4-7 cores are the tychoplanktonic *Fragilaria* spp. (Fig. 5) that are opportunistic species well adapted to nutrient-poor (oligotrophic) conditions and short growing seasons and therefore occur in great numbers as pioneer species in the early stages of lake evolution immediately following postglacial marine regression (Pienitz et al., 1991; Saulnier-Talbot and Pienitz, 2001).

High values of magnetic susceptibility and Ti and fine-grained sediment particle sizes in this section of all three cores are equally in accordance with increased glaciogenic sediment inputs

in the newly closed lake basin (Fig. 3 and 4). The black/brown laminated layers observed in this section likely represent meromictic lake conditions with saline waters trapped at the bottom of the lake (Fig. 2) that have been commonly reported from other coastal lakes in the Canadian Arctic (Cuven et al., 2011; Hove et al., 2006; Pienitz et al., 1991; Retelle, 1986). This is confirmed by high S contents used to infer anoxia in the deep-water layers due to euxinic conditions (Fig. 4b; Cuven et al., 2011). High Fe values were also observed. Specifically, microbial degradation of marine organic matter in oxygen-depleted deeper water due to the absence of convective circulation in the water column results in redox conditions that prevent bioturbation and favor the formation and preservation of laminated sediments.

5.1.3. Lacustrine phase (ca. 6000 cal. BP - present)

The lacustrine section marks the complete replacement of the basal saline waters and transition to the current freshwater state extending from ca. 6000 cal. BP to the present-day. The fossil diatom assemblage studies (Fig. 5) in cores Ni4-7 and Ni2-B using taxon-specific salinity tolerances were effective in identifying the exact stratigraphic position of the isolation contact in the cores, marked by an abrupt replacement of marine with freshwater diatoms directly inferring paleosalinity changes in the basin. This is further confirmed by the depleted, rather constant isotopic composition varying between $\delta^{18}\text{O}_{\text{diatom}} +21.4\text{‰}$ and $+24.0\text{‰}$ in Ni2-B core referring to freshwater conditions (Fig. 6). There is a trend towards lower $\delta^{18}\text{O}_{\text{diatom}}$ values towards the top of the section, which could reflect the Late Holocene summer cooling. This tendency is also visible in other lake diatom isotope records, i.e. on Kamchatka (Meyer et al., 2014) and near Lake Baikal (Kostrova et al., 2013, 2014).

Sediments in the lacustrine section consist of massive (Ni2-B) or laminated (Ni-MP and Ni4-7) deposits. The laminated facies in the Ni-MP and Ni4-7 cores likely reflect regular sediment influx, while the massive deposits in the Ni2-B core may be associated to irregular sedimentation influx with longer periods without deposition (Fig. 3). The latter period could be associated with the Neoglacial cold phase on Baffin Island that persisted from 6000 to 2000 ^{14}C BP years as documented in other Baffin Island lake records (e.g., Miller et al., 2005; Wolfe et al., 2000). Abrupt increases in MS and coarser-grained sediments in the Ni2-B core are probably due to the greater proportion of clastic sediments resulting from glacial erosion induced by temporary glacial readvances during Neoglacial cooling (Miller et al., 2005). Declines in primary production were likely caused by lower summer temperatures and shorter ice-free growing seasons (Fig. 3). However, this cooling trend was not observed in the $\delta^{18}\text{O}_{\text{diatom}}$ record. These shifts mark the onset of a glacio-lacustrine dominated environment at Nettilling Lake that had started as a brackish-lacustrine interphase (ca. 7300 to 6000 cal. BP) with the return to lower MS and increased primary production within the uppermost 10 cm of cores Ni-MP and Ni2-B. However, a subsequent in-depth investigation of the lacustrine phase is necessary in order to understand the limnological and sedimentological discrepancies apparent in different parts of the lake basin.

Despite its large size (5500 km²) and diversity with respect to local geology, topography and basin morphology, the development of Nettilling Lake does not differ much from that of other high latitude lake systems. Throughout the entire basin, the analyzed cores reveal about 10 cm of glaciomarine sediments and close to 30 cm of brackish water deposition. However, the immediate postglacial sediments have not been deposited at the same and constant supply rate everywhere in the basin. Major differences are apparent in the lacustrine phase where sedimentation rates appear to be highest in the south-central part of the lake basin at the Ni-MP

coring site, due to the geographic proximity to inflows from Amadjuak Lake, as well as the plume region that receives massive inflows from the Isurtuq River (Chapligin et al., 2016, in review, this issue).

6. Conclusions

This study presents the first multi-proxy postglacial environmental reconstruction of Mid- to Late Holocene (ca. 8300 cal. BP to present) paleogeographic and paleoenvironmental changes inferred from Nettilling Lake cores of southwestern Baffin Island. The main research results can be summarized as follows:

- Geochemical and biological proxies of three cores concurrently register initial postglacial marine influence. The sediment core records reveal a glaciomarine-lacustrine transition through paleosalinity shifts inferred from the elemental geochemistry using micro X-ray fluorescence, fossil diatom and foraminifer assemblages, as well as the oxygen isotopic record ($\delta^{18}\text{O}_{\text{diatom}}$) preserved in biogenic silica. The Nettilling Lake basin remained under postglacial marine influence until ca. 6000 cal. BP following the retreat of the LIS in the region after ca. 8300 cal. BP. Fluvial processes (runoff) supplied freshwaters and sediments leading to the progressive freshening and creation of the present-day ultra-oligotrophic lake system.
- *In situ* measured radiocarbon date of ca. 7400 cal. BP for the marine phase, suggests that Foxe Basin deglaciation happened a ca. 400 yrs earlier than previously thought.
- There is no additional evidence for a marine transgression via the Cumberland Sound as previously suggested by Blake (1966).
- Additional coring sites and radiocarbon dates at different elevations within the vast lake basin are necessary to further refine the rates of glacio-isostatic rebound for this remote Arctic region where paleogeographic data are extremely sparse.
- Our study presents the first $\delta^{18}\text{O}_{\text{diatom}}$ record from the eastern Canadian Arctic documenting the postglacial glaciomarine-lacustrine transition. It provides further evidence for the usefulness of $\delta^{18}\text{O}_{\text{diatom}}$ as an important new proxy for paleoenvironmental and paleoclimate reconstructions, in this case indicative of paleosalinity changes that are in line with changes in the lake water isotope composition.

Acknowledgments

This work is part of a Ph.D. research project funded through a Discovery research grant awarded to R. Pienitz from the Natural Sciences and Engineering Research Council (NSERC) of Canada, an NSERC Northern Supplement grant to R. Pienitz and P. Francus, the Arctic Development and Adaptation to Permafrost in Transition (ADAPT) NSERC-Discovery Frontiers program, the Northern Scientific Training Program (NSTP- Canadian Polar Commission), The Network of Centres of Excellence of Canada program ArcticNet, the NSERC-CREATE EnviroNord training program in Northern Environmental Sciences, funding obtained from Alfred Wegener Institute (AWI-Potsdam) and Bundesministerium für Bildung und Forschung (BMBF project number 01DM14009), as well as logistic support from Polar Continental Shelf program (PCSP project number 613-13 and 643-14) and Centre d'Études Nordiques (CEN). We would like to express our gratitude to Jim Leafloor and Pat Rakowski of the Canadian Wildlife Service (CWS) for allowing us to use their camp facilities at Nikku Island, Nunavut. We would also like to thank Rick Armstrong (Nunavut Research Institute, Iqaluit), Denis Sarrazin (CEN) and Steve Lodge (United Helicopters of Newfoundland) for their assistance in the field. We are grateful to Andrew Medeiros and Emilie Saulnier-Talbot for inspiring

discussions and Claudia Zimmermann for help in the laboratory. In addition, we thank Helga Kemnitz from the German Research Center for Geosciences for her SEM support.

References

- Abbott, M.B., Stafford Jr., T.W., 1996. Radiocarbon geochemistry of modern and ancient Arctic lake systems, Baffin Island, Canada. *Quat. Res.* 45, 300–311. <http://dx.doi.org/10.1006/qres.1996.0031>.
- ACIA, 2005. Arctic Climate Impact Assessment. Cambridge University Press, p. 1042.
- Alley, R.B., Andrews, J.T., Brigham-Grette, J., Clarke, G.K.C., Cuffey, K.M., Fitzpatrick, J.J., Funder, S., Marshall, S.J., Miller, G.H., Mitrovica, J.X., Muhs, D.R., Otto-Bliessner, B.L., Polyak, L., White, J.W.C., 2010. History of the Greenland Ice Sheet: paleoclimatic insights. *Quat. Sci. Rev.* 29, 1728–1756. <http://dx.doi.org/10.1016/j.quascirev.2010.02.007>.
- Antoniades, D., Crowley, C., Douglas, M.S.V., Pienitz, R., Andersen, D., Doran, P.T., Hawes, I., Pollard, W., Vincent, W.F., 2007. Abrupt environmental change in Canada's northernmost lake inferred from fossil diatom and pigment stratigraphy. *Geophys. Res. Lett.* 34, L18708. <http://dx.doi.org/10.1029/2007GL030947>.
- Antoniades, D., Hamilton, P.B., Douglas, M.S.V., Smol, J.P., 2008. Diatoms of North America. In: Bertalot, H.L. (Ed.), *Iconographia Diatomologica*, 17. A. R. G. Gantner Verlag K. G., p. 649.
- Axford, Y., Briner, J.P., Miller, G.H., Francis, D.R., 2009. Paleocological evidence for abrupt cold reversals during peak Holocene warmth on Baffin Island, Arctic Canada. *Quat. Res.* 71, 142–149. <http://dx.doi.org/10.1016/j.yqres.2008.09.006>.
- Barber, D.C., Dyke, A., Hillaire-Marcel, C., Jennings, A.E., Andrews, J.T., Kerwin, M.W., Bilodeau, B., McNeely, R., Southon, J., Morehead, M.D., Gagnon, J.-M., 1999. Forcing of the cold event of 8,200 years ago by catastrophic drainage of Laurentide lakes. *Nature* 400, 344–348. <http://dx.doi.org/10.1038/22504>.
- Blake, J.W., 1966. End moraines and deglaciation chronology in northern Canada with special reference southern Baffin Island. *Geol. Surv. Can.* 66–26.
- Bouchard, F., Francus, P., Pienitz, R., Laurion, I., 2011. Sedimentology and geochemistry of thermokarst ponds in discontinuous permafrost, subarctic Quebec, Canada. *J. Geophys. Res. Biogeosciences* 116, 1–14. <http://dx.doi.org/10.1029/2011JG001675>.
- Beaudoin, A., Pienitz, R., Francus, P., Zdanowicz, C., St-Onge, G., 2016. Paleoenvironmental reconstruction of the Nettilling Lake area (Nunavut, Canada): a multi-proxy analysis. *Holocene* (in review).
- Briner, J.P., Miller, G.H., Davis, P.T., Finkel, R.C., 2005. Cosmogenic exposure dating in arctic glacial landscapes: implications for the glacial history of northeastern Baffin Island, Arctic Canada. *Can. J. Earth Sci.* 42, 67–84. <http://dx.doi.org/10.1139/e04-102>.
- Brewer, T.S., Leng, M.J., Mackay, A.W., Lamb, A.L., Tyler, J.J., Marsh, N.G., 2008. Unravelling contamination signals in biogenic silica oxygen isotope composition; the role of major and trace element geochemistry. *J. Quat. Sci.* 23, 321–330. <http://dx.doi.org/10.1002/jqs.117>.
- Campeau, S., Pienitz, R., Héquette, A., 1999. Diatoms from the Beaufort Sea Coast, Southern Arctic Ocean (Canada). In: *Bibliotheca Diatomologica* 42. J. Cramer, Berlin/Stuttgart, p. 244.
- Chapligin, B., Leng, M.J., Webb, E., Alexandre, A., Dodd, J.P., Ijiri, A., Lücke, A., Shemesh, A., Abelmann, A., Herzschuh, U., Longstaffe, F.J., Meyer, H., Moschen, R., Okazaki, Y., Rees, N.H., Sharp, Z.D., Sloane, H.J., Sonzogni, C., Swann, G.E., Sylvestre, F., Tyler, J.J., Yam, R., 2011. Inter-laboratory comparison of oxygen isotope compositions from biogenic silica. *Geochim. Cosmochim. Acta* 75, 7242–7256. <http://dx.doi.org/10.1016/j.gca.2011.08.011>.
- Chapligin, B., Meyer, H., Bryan, A., Snyder, J., Kemnitz, H., 2012a. Assessment of purification and contamination correction methods for analysing the oxygen isotope composition from biogenic silica. *Chem. Geol.* 300–301, 185–199. <http://dx.doi.org/10.1016/j.chemgeo.2012.01.004>.
- Chapligin, B., Meyer, H., Friedrichsen, H., Marent, A., Sohns, E., Hubberten, H.W., 2010. A high-performance, safer and semi-automated approach for the $\delta^{18}\text{O}$ analysis of diatom silica and new methods for removing exchangeable oxygen. *Rapid Commun. Mass Spectrom.* 24, 2655–2664. <http://dx.doi.org/10.1002/rcm.4689>.
- Chapligin, B., Meyer, H., Swann, G.E.A., Meyer-Jacob, C., Hubberten, H.W., 2012b. A 250 ka oxygen isotope record from diatoms at Lake El'gygytgyn, far east Russian Arctic. *Clim. Past.* 8, 1621–1636. <http://dx.doi.org/10.5194/cp-8-1621-2012>.
- Chapligin, B., Narancic, B., Meyer, H., Pienitz, R., 2016. Palaeo-environmental gateways in the eastern Canadian Arctic - recent isotope hydrology and diatom oxygen isotopes from Nettilling Lake, Baffin Island, Canada. *Quat. Sci. Rev. Past. Gatew. Spec. issue* (in review).
- Croudace, I.W., Rindby, A., Rothwell, R.G., 2006. ITRAX: Description and Evaluation of a New Multi-function X-ray Core Scanner, pp. 51–63. <http://dx.doi.org/10.1144/GSL.SP.2006.267.01.04>.
- Cuven, S., Francus, P., Lamoureux, S., 2011. Mid to Late Holocene hydroclimatic and geochemical records from the varved sediments of East Lake, Cape Bounty, Canadian High Arctic. *Quat. Sci. Rev.* 30, 2651–2665. <http://dx.doi.org/10.1016/j.quascirev.2011.05.019>.
- De Angelis, H., Kleman, J., 2007. Palaeo-ice streams in the Foxe/Baffin sector of the Laurentide Ice Sheet. *Quat. Sci. Rev.* 26, 1313–1331. <http://dx.doi.org/10.1016/j.quascirev.2007.02.010>.
- Dyke, A.S., 2004. An outline of the deglaciation of North America with emphasis on

- central and northern Canada. *Quat. Glaciat. Chronol. Part II North Am.* 2b, 373–424.
- Dyke, A.S., Andrews, J.T., Clark, P.U., England, J.H., Miller, G.H., Shaw, J., Veillette, J.J., 2002. The Laurentide and Innuitian ice sheets during the Last Glacial Maximum. *Quat. Sci. Rev.* 21, 9–31. [http://dx.doi.org/10.1016/S0277-3791\(01\)00095-6](http://dx.doi.org/10.1016/S0277-3791(01)00095-6).
- Fallu, M.-A., Allaire, N., Pienitz, R., 2000. Freshwater Diatoms from Northern Québec and Labrador (Canada). Species-environment Relationships in Lakes of Boreal Forest, Forest-tundra and Tundra Regions. In: *Bibliotheca Diatomologica* 45. J. Cramer, Berlin/Stuttgart, p. 200.
- Fallu, M.-A., Pienitz, R., Walker, I.R., Lavoie, M., 2005. Paleolimnology of a shrub tundra lake and response of aquatic and terrestrial indicators to climatic change in Arctic Québec, Canada. *Palaeogeogr. Palaeoclimatol. Palaeoecol.* 3–4, 183–203. <http://dx.doi.org/10.1016/j.palaeo.2004.07.006>.
- Fisher, D.A., et al., 1998. Penny ice cap cores, Baffin Island, Canada, and the Wisconsin Foxe Dome Connection: two states of Hudson Bay ice cover. *Science* 279, 692–695. <http://dx.doi.org/10.1126/science.279.5351.692>.
- Fisher, D., Zheng, J., Burgess, D., Zdanowicz, C., Kinnard, C., Sharp, M., Bourgeois, J., 2012. Recent melt rates of Canadian arctic ice caps are the highest in four millennia. *Glob. Planet. Change* 84–85, 3–7. <http://dx.doi.org/10.1016/j.gloplacha.2011.06.005>.
- Ford, J.D., Gough, W.A., MacDonald, J., Irngaut, C., Qrunnut, K., 2009. Sea ice, climate change and community vulnerability in northern Foxe Basin, Canada. *Clim. Res.* 38, 137–154. <http://dx.doi.org/10.3354/cr00777>.
- Fulton, R.J., 1975. Quaternary Geology of Canada and Greenland. *Geol. Surv. Can. Geol. Can.* 1.
- Heiri, O., Lotter, A.F., Lemcke, G., 2001. Loss on ignition as a method for estimating organic and carbonate content in sediments: reproducibility and comparability of results. *J. Paleolimnol.* 25, 101–110. <http://dx.doi.org/10.1023/A:1008119611481>.
- Hove, P. Van, Belzile, C., Gibson, J.A., Vincent, W.F., 2006. Coupled landscape-lake evolution in High Arctic Canada. *Can. J. Earth Sci.* 43, 533–546. <http://dx.doi.org/10.1139/e06-003>.
- Jacobs, J.D., Grondin, L.D., 1988. The influence of an Arctic large-lakes system on mesoclimate in south-central Baffin Island, N.W.T., Canada. Department of Geography and Great Lakes Institute, University of Windsor. *Arct. Antarct. Alp. Res.* 20, 212–219.
- Jacobs, J.D., Headley, A.N., Maus, L.A., Mode, W.N., Simms, E.L., 1997. Climate and vegetation of the interior lowlands of southcentral Baffin Island: long-term stability at the low Arctic limit. *Arctic* 50, 167–177.
- Joynt III, E.H., Wolfe, A.P., 2001. Paleoenvironmental inference models from sediment diatom assemblages in Baffin Island lakes (Nunavut, Canada) and reconstruction of summer water temperature. *Can. J. Fish. Aquat. Sci.* 58, 1222–1243. <http://dx.doi.org/10.1139/f01-071>.
- Juggins, S., 2015. R Version 3.2.2. University of Newcastle, New castle upon Tyne.
- Kaufman, D.S., Ager, T.A., Anderson, N.J., Anderson, P.M., Andrews, J.T., Bartlein, P.J., Brubaker, L.B., Coats, L.L., Cwynar, L.C., Duvall, M.L., Dyke, A.S., Edwards, M.E., Eisner, W.R., Gajewski, K., Geirsdóttir, A., Hu, F.S., Jennings, A.E., Kaplan, M.R., Kerwin, M.W., Lozhkin, A.V., MacDonald, G.M., Miller, G.H., Mock, C.J., Oswald, W.W., Otto-Bliesner, B.L., Porinchu, D.F., Rühland, K., Smol, J.P., Steig, E.J., Wolfe, B.B., 2004. Holocene thermal maximum in the western Arctic (0–180°W). *Quat. Sci. Rev.* 23, 529–560. <http://dx.doi.org/10.1016/j.quascirev.2003.09.007>.
- Kaufman, D.S., Schneider, D.P., McKay, N.P., Ammann, C.M., Bradley, R.S., Briffa, K.R., Miller, G.H., Otto-Bliesner, B.L., Overpeck, J.T., Vinther, B.M., 2009. Recent warming reverses long-term arctic cooling. *Science* 325, 1236–1239. <http://dx.doi.org/10.1126/science.1173983>.
- Kostrova, S.S., Meyer, H., Chaplignin, B., Kossler, A., Bezrukova, E.V., Tarasov, P.E., 2013. Holocene oxygen isotope record of diatoms from Lake Kotokel (southern Siberia, Russia) and its palaeoclimatic implications. *Quat. Int.* 290–291, 21–34. <http://dx.doi.org/10.1016/j.quaint.2012.05.011>.
- Kostrova, S.S., Meyer, H., Chaplignin, B., Tarasov, P.E., Bezrukova, E.V., 2014. The last glacial maximum and late glacial environmental and climate dynamics in the Baikal region inferred from an oxygen isotope record of lacustrine diatom silica. *Quat. Int.* 348, 25–36. <http://dx.doi.org/10.1016/j.quaint.2014.07.034>.
- Krammer, K., Lange-Bertalot, H., 1986. Bacillariophyceae. 1. Teil : Naviculaceae. In: Ettl, H., Gärtner, G., Gerloff, J., Heynig, H., Mollenhauer, D. (Eds.), *Sü.wasserflora von Mitteleuropa, Band 2/1*. Gustav Fischer Verlag, Stuttgart/New York, p. 876.
- Krammer, K., Lange-Bertalot, H., 1988. Bacillariophyceae. 2. Teil : Bacillariaceae, Epithemiaceae, Surirellaceae. In: Ettl, H., Gerloff, J., Heynig, H., Mollenhauer, D. (Eds.), *Sü.wasserflora von Mitteleuropa, Band 2/2*. Gustav Fischer Verlag, Stuttgart/New York, p. 596.
- Krammer, K., Lange-Bertalot, H., 1991a. Bacillariophyceae. 3. Teil : Centrales, Fragilariaceae, Eunotiaceae. In: Ettl, H., Gerloff, J., Heynig, H., Mollenhauer, D. (Eds.), *Sü.wasserflora von Mitteleuropa, Band 2/3*. Gustav Fischer Verlag, Stuttgart/Jena, p. 576.
- Krammer, K., Lange-Bertalot, H., 1991b. Bacillariophyceae. 4. Teil : Achnantheaceae, Kritische Ergänzungen zu Navicula (Lineolatae) und Gomphonema. In: Ettl, H., Gärtner, G., Gerloff, J., Heynig, H., Mollenhauer, D. (Eds.), *Sü.wasserflora von Mitteleuropa, Band 2/4*. Gustav Fischer Verlag, Stuttgart/Jena, p. 437.
- Leclerc, A.J., Labeyrie, L., 1987. Temperature dependence of the oxygen isotopic fractionation between diatom silica and water. *Earth Planet. Sci. Lett.* 84, 69–74. [http://dx.doi.org/10.1016/0012-821X\(87\)90177-4](http://dx.doi.org/10.1016/0012-821X(87)90177-4).
- Maxwell, J.B., 1981. Climate regions of the Canadian Arctic islands. *Arctic* 34, 225–240. <http://dx.doi.org/10.14430/arctic2525>.
- McCave, I.N., Syvitski, J.P.M., 1991. Principles and methods of geological particle size analysis. In: Syvitski, J.P.M. (Ed.), *Principles, Methods and Application of Particle Size Analysis*. Cambridge University Press, p. 368.
- Meyer, H., Chaplignin, B., Hoff, U., Nazarova, L., Diekmann, B., 2014. Oxygen isotope composition of diatoms as Late Holocene climate proxy at Two-Yurts Lake, Central Kamchatka, Russia. *Glob. Planet. Change*. <http://dx.doi.org/10.1016/j.gloplacha.2014.04.008>.
- Miller, G.H., Mode, W.N., Wolfe, A.P., Sauer, P.E., Bennike, O., Forman, S.L., Short, S.K., Stafford, T.W., 1999. Stratified interglacial lacustrine sediments from Baffin Island, Arctic Canada: chronology and paleoenvironmental implications. *Quat. Sci. Rev.* 18, 789–810. [http://dx.doi.org/10.1016/S0277-3791\(98\)00075-4](http://dx.doi.org/10.1016/S0277-3791(98)00075-4).
- Miller, G.H., Wolfe, A.P., Briner, J.P., Sauer, P.E., Nesje, A., 2005. Holocene glaciation and climate evolution of Baffin Island, Arctic Canada. *Quat. Sci. Rev.* 24, 1703–1721. <http://dx.doi.org/10.1016/j.quascirev.2004.06.021>.
- Oliver, D.R., 1961. A limnological investigation of a large Arctic lake, Nettilling Lake, Baffin Island. *Arct. Inst. N. Am.* 17, 65–144. <http://dx.doi.org/10.14430/arctic3488>.
- Pienitz, R., Fedje, D., Poulin, M., 2003. Marine and Non-marine Diatoms from the Haida Gwaii Archipelago and Surrounding Coasts, Northeastern Pacific (Canada). In: *Bibliotheca Diatomologica* 48. J. Cramer, Berlin/Stuttgart, p. 146.
- Pienitz, R., Lortie, G., Allard, M., 1991. Isolation of lacustrine basins and marine regression in the Kuujuaq area (northern Québec), as inferred from diatom analysis. *Géogr. Phys. Quat.* 45, 155. <http://dx.doi.org/10.7202/032858ar>.
- Poulin, M., Bérard-Therriault, L., Cardinal, A., 1984a. Les diatomées benthiques de substrats durs des eaux marines et saumâtres du Québec. 1. Cocconeioideae. *Naturaliste Can* 111, 45–61.
- Poulin, M., Bérard-Therriault, L., Cardinal, A., 1984b. Les diatomées benthiques de substrats durs des eaux marines et saumâtres du Québec. 2. Tabellarioideae et Diatomoideae. *Naturaliste Can* 111, 275–295.
- Poulin, M., Bérard-Therriault, L., Cardinal, A., 1984c. Les diatomées benthiques de substrats durs des eaux marines et saumâtres du Québec. 3. Fragilarioideae. *Naturaliste Can* 111, 349–367.
- Prent, V.K., Grant, D.R., Rampton, V.N., 1968. Geological Survey of Canada. <http://dx.doi.org/10.4095/108979>. "A" Series Map 1253A, 1968; 1 sheet.
- Retelle, M.J., 1986. Stratigraphy and sedimentology of coastal lacustrine basins, Northeastern Ellesmere Island, N.W.T. *Géogr. Phys. Quat.* 40, 117. <http://dx.doi.org/10.7202/032632ar>.
- Rolland, N., Laroque, I., Francus, P., Pienitz, R., Laperriere, L., 2008. Holocene climate inferred from biological (Diptera: Chironomidae) analyses in a Southampton Island (Nunavut, Canada) lake. *Holocene* 18, 229–241. <http://dx.doi.org/10.1177/0959683607086761>.
- Saulnier-Talbot, É., Pienitz, R., 2001. Isolation au postglaciaire d'un bassin côtier près de Kuujuaqapik-Whapmagoostui, en Hudsonie (Québec): une analyse biostratigraphique diatomifère. *Géogr. Phys. Quat.* 55, 63–74. <http://dx.doi.org/10.7202/005662ar>.
- Saulnier-Talbot, É., Pienitz, R., Stafford, T.W., 2009. Establishing Holocene sediment core chronologies for northern Ungava lakes, Canada, using humic acids (AMS 14C) and 210Pb. *Quat. Geochronol.* 4, 278–287. <http://dx.doi.org/10.1016/j.quageo.2009.02.018>.
- Scherer, R.R., 1994. A new method for the determination of absolute abundance of diatoms and other silt-sized sedimentary particles. *J. Paleolimnol.* 12, 171–179. <http://dx.doi.org/10.1007/bf00678093>.
- Scott, D.B., Schell, T., Rochon, A., Blasco, S., 2008. Benthic foraminifera in the surface sediments of the Beaufort Shelf and slope, Beaufort Sea, Canada: Applications and implications for past sea-ice conditions. *J. Mar. Syst.* 74, 840–863. <http://dx.doi.org/10.1016/j.jmarsys.2008.01.008>.
- Smol, J.P., Wolfe, A.P., Birks, H.J.B., Douglas, M.S.V., Jones, V.J., Korhola, A., Pienitz, R., Rühland, K., Sorvari, S., Antoniadou, D., Brooks, S.J., Fallu, M.A., Hughes, M., Keatley, B.E., Laing, T.E., Michelutti, N., Nazarova, L., Nyman, M., Paterson, A.M., Perren, B., Quinlan, R., Rautio, M., Saulnier-Talbot, E., Siitonen, S., Solovieva, N., Weckström, J., 2005. Climate-driven regime shifts in the biological communities of arctic lakes. *Proc. Natl. Acad. Sci. U. S. A.* 102, 4397–4402. <http://dx.doi.org/10.1073/pnas.0500245102>.
- Snoeijs, P. (Ed.), 1993. *Intercalibration and Distribution of Diatom Species in the Baltic Sea*. Baltic Marine Biologists Publication 16a, vol. 1. Opulus Press, Uppsala, p. 129.
- Snoeijs, P., Balashova, N. (Eds.), 1998. *Intercalibration and Distribution of Diatom Species in the Baltic Sea*. Baltic Marine Biologists Publication 16e, vol. 5. Opulus Press, Uppsala, p. 144.
- Snoeijs, P., Kasperovicene, J. (Eds.), 1996. *Intercalibration and Distribution of Diatom Species in the Baltic Sea*. Baltic Marine Biologists Publication 16d, vol. 4. Opulus Press, Uppsala, p. 126.
- Snoeijs, P., Potapova, M. (Eds.), 1995. *Intercalibration and Distribution of Diatom Species in the Baltic Sea*. Baltic Marine Biologists Publication 16c, vol. 3. Opulus Press, Uppsala, p. 126.
- Snoeijs, P., Vilbaste, S. (Eds.), 1994. *Intercalibration and Distribution of Diatom Species in the Baltic Sea*. Baltic Marine Biologists Publication 16b, vol. 2. Opulus Press, Uppsala, p. 125.
- Stuiver, M., Polach, H.A., 1977. Discussion: reporting of 14C data. *Radiocarbon* 19, 355–363.
- Stuiver, M., Reimer, P.J., Braziunas, Thomas F., 1998. High-precision radiocarbon age calibration for terrestrial and marine samples, 40, 1127–1151.
- Swann, G.E.A., Leng, M.J., 2009. A review of diatom $\delta^{18}O$ in palaeoceanography. *Quat. Sci. Rev.* 28, 384–398. <http://dx.doi.org/10.1016/j.quascirev.2008.11.002>.
- Thomas, E.K., Axford, Y., Briner, J.P., 2008. Rapid 20th century environmental change on northeastern Baffin Island, Arctic Canada inferred from a multi-proxy

- lacustrine record. *J. Paleolimnol.* 40, 507–517. <http://dx.doi.org/10.1007/s10933-007-9178-y>.
- Thomas, E.K., Briner, J.P., Axford, Y., Francis, D.R., Miller, G.H., Walker, I.R., 2011. A 2000-yr-long multi-proxy lacustrine record from eastern Baffin Island, Arctic Canada reveals first millennium AD cold period. *Quat. Res.* 75, 491–500. <http://dx.doi.org/10.1016/j.yqres.2011.03.003>.
- Vickers, K.J., Ward, B.C., Utting, D.J., Telka, A.M., 2010. Deglacial reservoir age and implications, Foxe Peninsula, Baffin Island. *J. Quat. Sci.* 25, 1338–1346. <http://dx.doi.org/10.1002/jqs.1419>.
- Witkowski, A., 1994. Recent and Fossil Diatom Flora of the Gulf of Gdansk, Southern Baltic Sea : Origin, Composition and Changes of Diatom Assemblages during the Holocene. In: *Bibliotheca Diatomologica, Band 28*. J. Cramer, Berlin/Stuttgart, p. 312.
- Witkowski, A., Bertalot, H.L., Metzeltin, D., 2000. Diatoms flora of marine coasts I. In: Bertalot, H.L. (Ed.), *Iconographia Diatomologica 7*Koeltz Scientific Books, p. 925.
- Wolfe, A.P., Fréchette, B., Richard, P.J.H., Miller, G.H., Forman, S.L., 2000. Paleocology of a 90,000-year lacustrine sequence from Fog Lake, Baffin Island. *Arct. Can.* 19, 1677–1699.
- Wolfe, A.P., Smith, I.R.O.D., 2004. Geochronology of high latitude lake sediments. In: Pienitz, R., Douglas, M.S.V., Smol, J.P. (Eds.), *Long-term Environmental Change in Arctic and Antarctic Lakes, Developments in Paleoenvironmental Research, vol. 8*. Springer, Dordrecht, pp. 241–268.
- Zdanowicz, C., Smetny-Sowa, A., Fisher, D., Schaffer, N., Copland, L., Eley, J., Dupont, F., 2012. Summer melt rates on Penny Ice Cap, Baffin Island: past and recent trends and implications for regional climate. *J. Geophys. Res. Earth Surf.* 117, 1–21. <http://dx.doi.org/10.1029/2011JF002248>.